CBR anisotropy from inflation-induced gravitational waves in mixed radiation and dust cosmology

Scott Koranda* and Bruce Allen†
Department of Physics, University of Wisconsin - Milwaukee, P.O. Box 413, Milwaukee, Wisconsin 53201
(Received 18 October 1994)

We examine stochastic temperature fluctuations of the cosmic background radiation (CBR) arising via the Sachs-Wolfe effect from gravitational wave perturbations produced in the early universe. We consider spatially flat, perturbed FRW models that begin with an inflationary phase, followed by a mixed phase containing both radiation and dust. The scale factor during the mixed phase takes the form $a(\eta) = c_1\eta^2 + c_2\eta + c_3$, where c_i are constants. During the mixed phase the universe smoothly transforms from being radiation to dust dominated. We find analytic expressions for the graviton mode function during the mixed phase in terms of spheroidal wave functions. This mode function is used to find an analytic expression for the multipole moments $\langle a_l^2 \rangle$ of the two-point angular correlation function $C(\gamma)$ for the CBR anisotropy. The analytic expression for the multipole moments is written in terms of two integrals, which are evaluated numerically. The results are compared to multipoles calculated for models that are *completely* dust dominated at last scattering. We find that the multipoles $\langle a_l^2 \rangle$ of the CBR temperature perturbations for $l > 10$ are significantly larger for a universe that contains both radiation and dust at last scattering. We compare our results with recent, similar numerical work and find good agreement. The spheroidal wave functions may have applications to other problems of cosmological interest.

PACS number(s): 98.80.Cq, 98.80.Es

I. INTRODUCTION

This paper considers the effect of primordial gravitational waves on the cosmic background radiation (CBR). We consider spatially flat, perturbed Friedmann-Robertson-Walker (FRW) universes that begin with an early inflationary phase. As the universe rapidly expands, perturbations of the spatial geometry that are local in origin (e.g., thermal fluctuations) are quickly redshifted both in amplitude and wavelength. After sufficient inflation these perturbations are no longer visible to an observer; the only perturbations that remain visible within a Hubble sphere are quantum-mechanical zero-point fluctuations. Because these perturbations extend to arbitrarily high frequencies, they cannot be redshifted away. Since the only significant perturbations remaining after inflation are zero-point fluctuations, we assume that the initial state of the universe was the vacuum state appropriate to de Sitter space, containing only the quantum fluctuations and no additional excitations. As the universe continues to expand after inflation, these quantum fluctuations are redshifted to longer wavelengths and amplified; one may think of this in terms of particle (graviton) production (as we do), nonadiabatic amplification, or super-radiant scattering. In the present epoch the occupation numbers of the graviton modes are large. This is not surprising. It has been shown that one may treat the collective effects of primordial gravitational waves as being due to the presence of a stochastic background of classical gravitational waves, and since gravitons are bosons, such an interpretation is only possible if the occupation numbers are large.

Sachs and Wolfe [1] showed how gravitational wave perturbations result in CBR temperature anisotropy. As photons from the CBR propagate, the paths they follow are perturbed by the metric perturbation h_{ij}, which in this discussion is due entirely to primordial gravitational waves. The energies of the photons are perturbed, which results in temperature fluctuations from point to point on the celestial sphere. These temperature fluctuations are usually characterized by the two-point angular correlation function $C(\gamma)$ defined on the celestial sphere. Here γ is the angle between two points on the sphere. Most often the two-point angular correlation function is expanded in terms of Legendre polynomials, and the expansion coefficients or multipole moments are calculated. For a derivation of the angular correlation function for spatially flat cosmologies see the recent paper by Allen and Koranda [2]. Henceforth we will assume that the reader is familiar with this paper, which contains a detailed review of previous work on this problem, a comprehensive discussion of the physical motivation, and a detailed and self-contained "first-principles" calculation.

Early work on this subject [3–6] assumed that the universe was completely dust dominated at last scattering when the CBR decoupled, as did recent work by White [7] which presented a concise derivation of the formula for the multipole moments due to tensor perturbations. Also recently, Grishchuk has adapted the terminology and techniques of quantum optics to the analysis [8].

*Electronic address: skoranda@dirac.phys.uwm.edu
†Electronic address: ballen@dirac.phys.uwm.edu

Grishchuk stresses the importance of the phase correlations between the modes of the metric perturbations. A similar analysis by Allen and Koranda [2] using standard "quantum field theory in curved space" techniques found equivalent results. We also showed that the now standard formula given by Abbott and Wise [5] and Starobinsky [6] for the lth multipole moment is a long-wavelength approximation to an exact formula. Both the work by Grishchuk and by Allen and Koranda assumed that the universe was completely dust dominated at last scattering.

The first authors to consider the CBR anisotropy (within the framework of the Sachs-Wolfe effect) for a universe that was *not* completely dust dominated at last scattering were Turner, White, and Lidsey [9]. They used a "transfer function" to express the solutions of the wave equation for the gravitational wave amplitude in terms of the standard long-wavelength formula given by Abbott and Wise. They found that the standard formula, which assumes that the universe is *completely* dust dominated at last scattering, consistently underestimates the contribution of gravitational waves to the CBR anisotropy. More recent work by Ng and Speliotopoulos [10] used numerical methods to integrate the wave equation and found similar results. Neither of these studies used analytic expressions for the gravitational wave amplitude (or, equivalently, the graviton mode function).

Other work has been done which does not directly use the Sachs-Wolfe formula to calculate the anisotropy due to gravitational waves. Crittenden *et al.* [11] numerically evolved the photon distribution function using first-order perturbation theory of the general relativistic Boltzmann equation for radiative transfer, and included a Thomson scattering source term. Dodelson, Knox, and Kolb [12] have done a similar numerical analysis. Both found that the standard formula of Abbott and Wise is only accurate for small l multipole moments, and consistently underestimates the contribution of the gravitational waves to the CBR anisotropy for higher l moments. A number of papers [13–17] have examined whether the different l dependences of the scalar and tensor contributions to the multipole moments permit one to distinguish the signal from the tensor perturbations from that of the scalar perturbations. More recently Knox and Turner have suggested [18] that a combination of full-sky measurements of the CBR anisotropy on angular scales of 3° and 0.5° might enable one to detect the primordial gravitational or tensor perturbations. For these purposes one must understand in detail the contribution of gravitational waves to the multipole moments $\langle a_l^2 \rangle$ for moments with l as large as 200.

In this paper we give the first correct analytic expression for the graviton mode function in a cosmology that transforms smoothly from being radiation to dust dominated. (We correct a minor error in earlier work by Sahni [19] and Nariai [20] which claims to find an analytic expression for the mode function.) We use this analytic expression and the Sachs-Wolfe formula to find an analytic expression for the multipole moments $\langle a_l^2 \rangle$ of the angular correlation function $C(\gamma)$. The analytic expression for the multipole moments is written in terms of two integrals; we use numerical methods to evaluate these integrals, and report numerical values for the multipole moments. We compare our results with those mentioned above, and find good agreement.

The paper is organized as follows. In Sec. II we reproduce general expressions for the angular correlation function derived in [2], and explain how one uses these formulas to calculate the multipole moments for any spatially flat, inflationary cosmological model. In Sec. III we introduce our cosmological model, which "begins" with an infinite de Sitter phase followed by a mixed phase that contains both radiation and dust. Early in the mixed phase the universe is radiation dominated; later it transforms smoothly from being radiation dominated to dust dominated. In Sec. IV we solve the massless Klein-Gordon equation (or wave equation) for the graviton mode function. During the mixed phase the solutions to the wave equation are expressed in terms of spheroidal wave functions. The multipole moments are calculated in Sec. V using the graviton mode function determined in Sec. IV. An analytic expression for the moments is given in terms of two integrals, which are then evaluated numerically. In Appendix A we discuss the spheroidal wave functions. The differential equation of spheroidal wave functions is introduced and its solutions examined. We introduce a useful notation for the spheroidal wave functions, and give a practical method for evaluating them. Appendix B describes the numerical techniques used to evaluate the spheroidal wave functions and the two multipole moment integrals. Finally in Appendix C we show that the multipole moments for a general spacetime are formally (ultraviolet) divergent. The divergence is removed by introducing a physically motivated cutoff graviton wave number $k_{\max}$.

Throughout this paper we use units where the speed of light $c = 1$. We retain Newton's gravitational constant G and Planck's constant $\hbar$ explicitly.

II. ANGULAR CORRELATION FUNCTION

We consider only the anisotropy of the cosmic background radiation (CBR) arising via the Sachs-Wolfe effect [1] from tensor perturbations (gravitational waves). The anisotropy is characterized by the two-point angular correlation function $C(\gamma)$, where γ is the angle between two points located on the celestial sphere. The correlation function may be expanded in terms of Legendre polynomials as

$$C(\gamma) = \left\langle \frac{\delta T}{T}(0) \frac{\delta T}{T}(\gamma) \right\rangle = \sum_{l=0}^{\infty} \frac{(2l+1)}{4\pi} \langle a_l^2 \rangle P_l(\cos\gamma). \tag{2.1}$$

The expansion coefficients $\langle a_l^2 \rangle$ are referred to as the multipole moments. The multipole moments are given in terms of an integral over graviton wave number k:

$$\langle a_l^2 \rangle \equiv 4\pi^2 (l+2)(l+1)l(l-1) \int_0^{\infty} \frac{dk}{k} |I_l(k)|^2. \tag{2.2}$$

Strictly speaking, the integral above is (ultraviolet) divergent, and should be cut off at some large wave number $k_{\max}$ rather then extending to infinity. This ultraviolet divergence and cutoff are discussed in detail in Appendix C. [Note that Eq. (2.67) of Ref. [2] is formally ultraviolet divergent and should also be cut off at some $k_{\max}$.] The function $I_l(k)$ in (2.2) is proportional to the Sachs-Wolfe integral along null geodesics, and is given by

$$I_l(k) \equiv \int_0^{\eta_0-\eta_{\rm LS}} d\lambda\, F(\lambda,k)\frac{j_l(k(\eta_0-\eta_{\rm LS}-\lambda))}{k(\eta_0-\eta_{\rm LS}-\lambda)^2}. \quad (2.3)$$

Here $\eta_{\rm LS}$ is the time of last scattering, and η_0 is the conformal time today. The function $j_l(z)$ is a spherical Bessel function of the first kind [21]. The function $F(\lambda,k)$ is proportional to the first derivative of the graviton mode function $\phi(\eta,k)$, and is defined by

$$F(\lambda,k) \equiv k^{1/2}\left[\frac{\partial}{\partial\eta}\phi(\eta,k)\right]_{\eta=\eta_{\rm LS}+\lambda}. \quad (2.4)$$

The graviton mode function obeys the massless Klein-Gordon or wave equation

$$\ddot{\phi} + 2\frac{\dot{a}(\eta)}{a(\eta)}\dot{\phi} + k^2\phi = 0, \quad (2.5)$$

where $a(\eta)$ is the scale factor and

$$\cdot \equiv \frac{\partial}{\partial\eta}. \quad (2.6)$$

The mode function must satisfy the Wronskian normalization condition

$$\{\phi(\eta,k)\dot{\phi}^*(\eta,k) - \phi^*(\eta,k)\dot{\phi}(\eta,k)\} = \frac{2i\hbar G}{\pi^2 a^2(\eta)}. \quad (2.7)$$

[Note that there is a sign error in the first term of Eq. (3.10) of Ref. [2]. As a result the right-hand side of Eqs. (3.11)–(3.15) and (3.19) should have the opposite sign.] The only physical input required is the choice of an initial quantum state for the gravitational field, which amounts to a choice of boundary conditions for the wave equation (2.5).

These formulas for the angular correlation function are very general; a detailed and complete derivation is given in [2]. To calculate the correlation function (or equivalently the multipole moments) for any particular cosmological model, one need only to solve the wave equation (2.5) for the graviton mode function, and substitute into the formulas (2.1)–(2.4).

III. COSMOLOGICAL MODEL

The spacetime considered here is a spatially flat, perturbed FRW universe. The metric is

$$ds^2 = a^2(\eta)\{-d\eta^2 + [\delta_{ij} + h_{ij}(\eta,x^k)]dx^i dx^j\}, \quad (3.1)$$

where δ_{ij} is the flat metric of R^3, η is the conformal time, and $a(\eta)$ is the cosmological length scale or scale factor. The scale factor satisfies the Einstein equations

$$\frac{\dot{a}^2(\eta)}{a^4(\eta)} = \frac{8\pi G}{3}\rho(\eta) \text{ and } \frac{\ddot{a}(\eta)}{a^3(\eta)} - \frac{\dot{a}^2(\eta)}{a^4(\eta)} = -\frac{4\pi G}{3}[\rho(\eta)+3P(\eta)], \quad (3.2)$$

where $\rho(\eta)$ is the energy density and $P(\eta)$ the pressure of the cosmological fluid. The metric perturbation h_{ij} is assumed to be small; in the limit as h_{ij} vanishes the spacetime is an unperturbed FRW universe. We have chosen a gauge so that the tensor perturbation h_{ij} has only spatial components.

In the absence of the metric perturbation h_{ij}, the background spacetime is a spatially flat FRW universe. Since the spacetime is spatially flat, the density parameter Ω_0, which is the ratio of the present-day energy density ρ_0 to the critical energy density required to produce a spatially flat universe, is equal to unity:

$$\Omega_0 = \frac{8\pi G\rho_0}{3H_0^2} = 1. \quad (3.3)$$

To specify the model, we need to give the scale factor $a(\eta)$. We do this in such a way that the model is completely defined by the minimal set of free parameters given in Table I. *All* our results, including the final expression (5.2), can be expressed in terms of this minimal set of parameters. For clarity, we often define auxiliary quantities and express results in terms of them; the auxiliary quantities can be expressed in terms of the parameters in Table I. In typical inflationary models,

TABLE I. List of free parameters that define the cosmological model.

Parameter	Units	Range	Description
H_0	Length^{-1}	$H_0 > 0$	Present-day Hubble expansion rate
$Z_{\rm LS}$	Dimensionless	$Z_{\rm LS} > 0$	Redshift at last scattering of CBR
$Z_{\rm eq}$	Dimensionless	Unrestricted	Redshift at equal matter-radiation energy density
$Z_{\rm end}$	Dimensionless	$Z_{\rm end} > Z_{\rm eq}, Z_{\rm LS}$	Redshift at end of de Sitter inflation

the free parameters in Table I have values of order H_0 between 50 and 100 $\mathrm{km\,s^{-1}\,Mpc^{-1}}$, $100 < Z_{\rm LS} < 1500$, $2\times10^3 < Z_{\rm eq} < 2\times10^4$, and $10^{20} < Z_{\rm end}$. For a review of inflationary cosmology see Ref. [22].

A. Inflationary or de Sitter phase

Our cosmological model passes through two phases. The first phase is a de Sitter or inflationary phase. During the de Sitter phase the universe expands exponentially [expressed in terms of *comoving* time t, the scale factor behaves like $a(t) \propto e^{Ht}$, where H is the Hubble constant]. In terms of conformal time, the scale factor is

$$a(\eta) = a(\eta_{\rm end})\left(2 - \frac{\eta}{\eta_{\rm end}}\right)^{-1} \quad \text{for } \eta \le \eta_{\rm end}, \tag{3.4}$$

where $\eta_{\rm end}$ is the conformal time at the end of the de Sitter phase. In terms of the parameters listed in Table I,

$$a(\eta_{\rm end}) = (1+Z_{\rm end})^{-1}, \tag{3.5}$$

$$\begin{aligned}\eta_{\rm end} &= H_0^{-1}\left[\frac{(2+Z_{\rm eq})}{(2+Z_{\rm eq}+Z_{\rm end})(1+Z_{\rm end})}\right]^{1/2} \\ &\approx H_0^{-1}\frac{\sqrt{Z_{\rm eq}}}{Z_{\rm end}},\end{aligned} \tag{3.6}$$

where we have set the scale factor today, $a(\eta_0) = 1$. During the de Sitter phase the energy density $\rho_{\rm dS}$ is constant and given by

$$\begin{aligned}\rho_{\rm dS} &= \frac{3}{8\pi G}\frac{\dot a^2(\eta_{\rm end})}{a^4(\eta_{\rm end})} \\ &= \frac{3H_0^2}{8\pi G}\frac{(1+Z_{\rm end})^3}{(2+Z_{\rm eq})}(2+Z_{\rm eq}+Z_{\rm end}) \\ &\approx \frac{3}{8\pi G}H_0^2\frac{Z_{\rm end}^4}{Z_{\rm eq}} = \frac{Z_{\rm end}^4}{Z_{\rm eq}}\rho_0.\end{aligned} \tag{3.7}$$

The pressure during the de Sitter phase is negative and constant, and is given by

$$P_{\rm dS} = -\rho_{\rm dS}. \tag{3.8}$$

The de Sitter phase is followed by a mixed phase.

B. Mixed radiation and dust phase

Immediately following the de Sitter phase is a mixed phase containing both dust and radiation. The scale factor is

$$a(\eta) = a(\eta_{\rm end})\left[\frac{1}{4}\left(\frac{\xi}{1+\xi}\right)\left(\frac{\eta}{\eta_{\rm end}} - 1\right)^2 + \frac{\eta}{\eta_{\rm end}}\right] \quad \text{for } \eta \ge \eta_{\rm end}. \tag{3.9}$$

The constant ξ is defined in terms of the free parameters by

$$\xi = \frac{1+Z_{\rm eq}}{1+Z_{\rm end}}. \tag{3.10}$$

The stress-energy tensor is that of a perfect fluid with energy density

$$\rho(\eta) = \rho_{\rm dust}(\eta) + \rho_{\rm rad}(\eta) \text{ for } \eta \ge \eta_{\rm end}, \tag{3.11}$$

where the energy density for the dust $\rho_{\rm dust}(\eta)$ and for the radiation $\rho_{\rm rad}(\eta)$ are

$$\rho_{\rm dust}(\eta) = \frac{\rho_{\rm eq}}{2}\frac{a^3(\eta_{\rm eq})}{a^3(\eta)}, \tag{3.12}$$

$$\rho_{\rm rad}(\eta) = \frac{\rho_{\rm eq}}{2}\frac{a^4(\eta_{\rm eq})}{a^4(\eta)}. \tag{3.13}$$

Here $\rho_{\rm eq} = \rho(\eta_{\rm eq})$ is the energy density at conformal time $\eta_{\rm eq}$, when the dust and radiation energy densities are equal, and is given by

$$\rho_{\rm eq} = \frac{3H_0^2}{4\pi G}\frac{(1+Z_{\rm eq})^4}{(2+Z_{\rm eq})} \approx 2\left(\frac{Z_{\rm eq}}{Z_{\rm end}}\right)^4\rho_{\rm dS} \approx 2{Z_{\rm eq}}^3\rho_0. \tag{3.14}$$

The pressure of the cosmological fluid $P(\eta)$ is

$$P(\eta) = P_{\rm rad}(\eta) = P_{\rm eq}\frac{a^4(\eta_{\rm eq})}{a^4(\eta)} \text{ for } \eta \ge \eta_{\rm end}, \tag{3.15}$$

where the pressure at dust-radiation equality $P_{\rm eq}$ is

$$P_{\rm eq} = P(\eta_{\rm eq}) = \frac{\rho_{\rm eq}}{6}. \tag{3.16}$$

By inspection of (3.13), (3.15), and (3.16) one sees that

$$P(\eta) = P_{\rm rad}(\eta) = \frac{1}{3}\rho_{\rm rad}(\eta), \tag{3.17}$$

which is the relation between the pressure and energy density one would expect since the dust has zero pressure and the pressure is due entirely to the radiation present. The scale factor at $\eta_{\rm eq}$ is

$$a(\eta_{\rm eq}) = (1+Z_{\rm eq})^{-1}. \tag{3.18}$$

One can express $\eta_{\rm eq}$ in terms of the conformal time at the end of the de Sitter phase $\eta_{\rm end}$ and the constant ξ as

$$\eta_{\rm eq} = \frac{\eta_{\rm end}}{\xi}[2\sqrt{2(1+\xi)} - 2 - \xi] \approx H_0^{-1}\frac{2(\sqrt{2}-1)}{\sqrt{Z_{\rm eq}}}. \tag{3.19}$$

For $\eta \ll \eta_{\rm eq}$ the energy density (3.11) varies as $\rho(\eta) \sim a^{-4}(\eta)$ and the cosmological model is radiation dominated, and for $\eta \gg \eta_{\rm eq}$ the energy density varies as $\rho(\eta) \sim a^{-3}(\eta)$ and the model is dust dominated. The model makes a smooth transition at $\eta = \eta_{\rm eq}$ from being radiation to dust dominated.

IV. GRAVITON MODE FUNCTION

To calculate the multipole moments for the cosmological model described above, one must first solve the wave equation (2.5) for the graviton mode function. We first solve for the "natural" positive- and negative-frequency mode functions during both the de Sitter and the mixed phases. We then make an appropriate choice of initial mode function during the de Sitter phase. This choice of initial mode function completely determines the graviton mode function for all later times. We express the mode function at later times using Bogolubov coefficient notation.

A. de Sitter phase

The solution to the wave equation (2.5) for the de Sitter phase can be expressed in terms of spherical Hankel functions. The scale factor during the de Sitter phase is given in (3.4). By making a change of the dependent variable

$$\chi(\eta,k) = (\eta - 2\eta_{\rm end})^{-2}\phi(\eta,k) \tag{4.1}$$

and a change of the independent variable

$$z = k(\eta - 2\eta_{\rm end}), \tag{4.2}$$

the wave equation can be expressed in the form

$$\frac{d^2\chi}{dz^2} + \frac{2}{z}\frac{d\chi}{dz} + \left(1 - \frac{2}{z^2}\right)\chi = 0. \tag{4.3}$$

This is Bessel's differential equation, and the solutions are spherical Bessel or Hankel functions [21]. Using the normalization condition (2.7) one obtains, for the positive-frequency mode function during the de Sitter phase,

$$\phi^{(+)}_{\rm dS}(\eta,k) = -i\sqrt{\frac{8}{3\pi}\frac{\rho_{\rm dS}}{\rho_P}}\, e^{-ik\eta_{\rm end}}\, \eta_{\rm end}^2 k^{1/2}\frac{a^2(\eta_{\rm end})}{a^2(\eta)} \times h_1^{(2)}(k(\eta - 2\eta_{\rm end})), \tag{4.4}$$

where $h_1^{(2)}(z)$ is a spherical Hankel function of the second kind [21], and $\rho_P = 1/\hbar G^2 \approx 5 \times 10^{93}$ g/cm^3 is the Planck energy density. The negative-frequency mode function during the de Sitter phase $\phi^{(-)}_{\rm dS}(\eta,k)$ is just the complex conjugate of the positive-frequency mode function (4.4). The positive- and negative-frequency mode functions form a complete solution to the wave equation for the de Sitter phase.

B. Mixed radiation and matter phase

The wave equation during the mixed radiation and dust phase ($\eta > \eta_{\rm end}$) can be cast in the form of the spheroidal wave function differential equation. By making a change of the dependent variable

$$\chi(\eta,k) \equiv a^{1/2}(\eta)\phi(\eta,k), \tag{4.5}$$

the wave equation (2.5) becomes

$$\ddot{\chi} + \frac{\dot{a}(\eta)}{a(\eta)}\dot{\chi} + \left(k^2 - \frac{1}{4}\frac{\dot{a}^2(\eta)}{a^2(\eta)} - \frac{1}{2}\frac{\ddot{a}(\eta)}{a(\eta)}\right)\chi = 0. \tag{4.6}$$

One may define a new independent variable

$$x \equiv \sqrt{1 + \frac{a(\eta)}{a(\eta_{\rm eq})}}, \tag{4.7}$$

so that

$$\frac{dx}{d\eta} = \frac{1}{2x}\frac{\dot{a}(\eta)}{a(\eta_{\rm eq})}. \tag{4.8}$$

Using (4.7) and (4.8) one may write the wave equation (4.6) in the form

$$\frac{d^2\chi}{dx^2} + \left[2x\frac{\ddot{a}(\eta)a(\eta_{\rm eq})}{\dot{a}^2(\eta)} - \frac{1}{x} + 2x\frac{a(\eta_{\rm eq})}{a(\eta)}\right]\frac{d\chi}{dx} + \left[4k^2x^2\frac{a^2(\eta_{\rm eq})}{\dot{a}^2(\eta)} - x^2\frac{a^2(\eta_{\rm eq})}{a^2(\eta)} - 2x^2\frac{\ddot{a}(\eta)a^2(\eta_{\rm eq})}{\dot{a}^2(\eta)a(\eta)}\right]\chi = 0. \tag{4.9}$$

This expression can be simplified using the Einstein equations (3.2), along with (3.11) and (4.7). One can show that

$$\dot{a}^2(\eta) = 2x^2\ddot{a}(\eta)a(\eta_{\rm eq}), \tag{4.10}$$

and using this expression one may write the wave equation (4.9) as

$$\frac{d^2\chi}{dx^2} + 2x\frac{a(\eta_{\rm eq})}{a(\eta)}\frac{d\chi}{dx} + \left[2k^2\frac{a(\eta_{\rm eq})}{\ddot{a}(\eta)} - x^2\frac{a^2(\eta_{\rm eq})}{a^2(\eta)} - \frac{a(\eta_{\rm eq})}{a(\eta)}\right]\chi = 0. \tag{4.11}$$

Since, from (4.7),

$$\frac{a(\eta_{\rm eq})}{a(\eta)} = \frac{1}{x^2 - 1}, \tag{4.12}$$

and, from (3.9) and (3.10),

$$\frac{\ddot{a}(\eta)}{a(\eta_{\rm eq})} = \frac{1}{2\eta_{\rm end}{}^2}\left(\frac{\xi^2}{1+\xi}\right), \tag{4.13}$$

the wave equation becomes

$$\frac{d^2\chi}{dx^2} - \frac{2x}{(1-x^2)}\frac{d\chi}{dx} + \left\{\frac{2}{(1-x^2)} + 4\kappa - \frac{1}{(1-x^2)^2}\right\}\chi = 0. \tag{4.14}$$

Here κ is defined by

$$\kappa \equiv \left(\frac{1+\xi}{\xi^2}\right) k^2 {\eta_{\rm end}}^2 = \frac{4\pi^2}{\lambda_0^2 H_0^2} \frac{(2+Z_{\rm eq})}{(1+Z_{\rm eq})^2} \approx \frac{4\pi^2}{\lambda_0^2 H_0^2 Z_{\rm eq}}, \tag{4.15}$$

where λ_0 is the *present-day* wavelength of the mode with wave number k. For the multipole moments of interest, $l \in [2, 1000]$, the contributions typically come from wavelengths in the range $\kappa \in [10^{-3}, 10^3]$. This form of the wave equation is the spheroidal wave function differential equation (A1), which is discussed in detail in Appendix A.

The solutions to the wave equation (2.5) during the mixed phase can be expressed in terms of spheroidal wave functions. By inspection of (4.7) one sees that $x > 1$, and so the possible solutions to the wave equation (4.14) may be expressed as sums of any pair of

$$\chi(x,\kappa) = {}^j\Sigma_2^1(x,\kappa), \quad j = 1,2,3,4, \tag{4.16}$$

where ${}^j\Sigma_2^1(x,\kappa)$ is a spheroidal wave function. *Our notation for the spheroidal wave functions differs from that used in Ref.* [19]. *In particular the indices on* ${}^j\Sigma_\lambda^\mu(x,\kappa)$ *have a different meaning than those used in* [19]. Our notation for the spheroidal wave functions and our motivation for using this notation are discussed in detail in Appendix A. Using (4.5), (4.16), the normalization condition (2.7), and the Wronskian relation (A22), one obtains a positive-frequency mode function during the mixed phase:

$$\phi^{(+)}_{\rm mix}(\eta,k) = -2i\sqrt{\frac{8}{3\pi}\frac{\rho_{\rm dS}}{\rho_P}\frac{a(\eta_{\rm end})}{a(\eta)}\left(\frac{1+\xi}{\xi}\right)} \times \eta_{\rm end}^2 k^{1/2}\, {}^4\Sigma_2^1(x,\kappa). \tag{4.17}$$

Note that x is a function of the conformal time η and κ depends on the wave number k. The negative-frequency mode function $\phi^{(-)}_{\rm mix}(\eta,k) = [\phi^{(+)}_{\rm mix}(\eta,k)]^*$ is just the complex conjugate of the positive-frequency mode function. The positive- and negative-frequency mode functions form a complete solution to the wave equation during the mixed radiation and matter phase. Note that the choice of graviton mode function during the de Sitter phase completely determines the mode function at all later times. Thus, the choice (4.17) of "positive frequency" during the mixed phase is unimportant.

C. Graviton mode function expressed using Bogolubov coefficient notation

The choice of mode function during the de Sitter phase completely determines the mode function at all later times. This is because a solution to the wave equation depends only on the values of ϕ and $\dot\phi$ on a spacelike Cauchy surface (i.e., a surface of constant η). We choose the mode function during the de Sitter phase to be the pure positive-frequency de Sitter solution (4.4). This is the unique solution corresponding to a de Sitter–invariant vacuum state with the same (Hadamard) short distance behavior as one would find in Minkowski space [23]. Having made this choice for the mode function during the de Sitter phase, the mode function for all times is

$$\phi(\eta,k) = \begin{cases} \phi^{(+)}_{\rm ds}(\eta,k), & \eta \le \eta_{\rm end},\ \text{de Sitter phase}, \\ \alpha(k\eta_{\rm end})\phi^{(+)}_{\rm mix}(\eta,k) + \beta(k\eta_{\rm end})\phi^{(-)}_{\rm mix}(\eta,k), & \eta \ge \eta_{\rm end},\ \text{mixed phase}, \end{cases} \tag{4.18}$$

where α and β are Bogolubov coefficients.

The Bogolubov coefficients are determined by requiring that the mode function and its first derivative be continuous at $\eta = \eta_{\rm end}$. One obtains

$$\alpha(k\eta_{\rm end}) = \sqrt{\frac{1+\xi}{\xi}}\left\{\left[\frac{\xi}{\sqrt{1+\xi}}\,{}^3\Sigma_2^{1\prime}(x_1,\kappa) - {}^3\Sigma_2^1(x_1,\kappa)\right]\left(\frac{i}{2} - \frac{1}{2k\eta_{\rm end}}\right) - k\eta_{\rm end}\,{}^3\Sigma_2^1(x_1,\kappa)\right\},$$

$$\beta(k\eta_{\rm end}) = \sqrt{\frac{1+\xi}{\xi}}\left\{\left[\frac{\xi}{\sqrt{1+\xi}}\,{}^4\Sigma_2^{1\prime}(x_1,\kappa) - {}^4\Sigma_2^1(x_1,\kappa)\right]\left(\frac{i}{2} - \frac{1}{2k\eta_{\rm end}}\right) - k\eta_{\rm end}\,{}^4\Sigma_2^1(x_1,\kappa)\right\}. \tag{4.19}$$

The prime in (4.19) is defined by

$${}^j\Sigma_\lambda^{\mu\prime}(x_1,\theta) \equiv \left[\frac{\partial}{\partial z}\,{}^j\Sigma_\lambda^\mu(z,\theta)\right]_{z=x_1}, \tag{4.19}$$

where

$$x_1 \equiv \sqrt{1 + \frac{a(\eta_{\rm end})}{a(\eta_{\rm eq})}} = \sqrt{1+\xi}. \tag{4.20}$$

Using the Wronskian relation for the spheroidal wave functions (A22) one can easily verify that

$$|\alpha(k\eta_{\rm end})|^2 - |\beta(k\eta_{\rm end})|^2 = 1. \tag{4.21}$$

We stress again that *the choice of graviton mode function during the de Sitter phase completely determines the mode function at all later times.* Thus, the choice of "positive frequency" during the mixed phase is unimportant.

Had we chosen a different solution to the wave equation during the mixed phase to call "positive frequency," then the Bogolubov coefficients (4.19) would be different in such a way so that the mode function (4.18) *would be the same.*

V. MULTIPOLE MOMENTS

Having determined the graviton mode function for our cosmological model, we may calculate the angular correlation function $C(\gamma)$ or, equivalently, the multipole moments $\langle a_l^2 \rangle$. We simply substitute the graviton mode function (4.18) into the formulas (2.1)–(2.4).

A. Analytical results

The graviton mode function (4.18) is exact; no approximations (i.e., long wavelength) have been made. One may directly substitute the mode function into the formulas (2.1)–(2.4) to obtain an exact expression for the multipole moments; because the arguments of the spheroidal wave functions in (4.18) are functions themselves, however, the result is complicated and not very illuminating. In typical inflationary models, the amount of expansion is very large. If one takes the limit $Z_{\rm end} \to \infty$, then $\xi \to 0$, as may be seen from (3.10). This allows one to write a fairly compact expression for the multipole moments; after substituting the mode function (4.18) into the formulas (2.1)–(2.4), one may collect together terms in the expression for the multipole moments $\langle a_l^2 \rangle$ which are the same order in ξ. Then in the limit as $Z_{\rm end} \to \infty$ and $\xi \to 0$, one may consider only the leading term. The leading term, which is $O(\xi^0)$, is given below in (5.2). The neglected terms are $O(\xi^1)$ or greater. For typical inflationary models one has $Z_{\rm end} \gtrsim 10^{20}$ and $Z_{\rm eq} \approx 10^4$, so that $\xi \lesssim 10^{-16}$. So the expression (5.2) is quite accurate for most cosmological models, since the neglected terms are very small.

The expressions for the multipole moments $\langle a_l^2 \rangle$ are fairly simple. After substituting the mode function (4.18) into the formulas (2.1)–(2.4), and making the same changes of variable as in Sec. IV B, i.e.,

$$x \equiv \sqrt{1 + \frac{a(\eta)}{a(\eta_{\rm eq})}} \quad \text{and} \quad \kappa \equiv \left(\frac{1+\xi}{\xi^2}\right) k^2 \eta_{\rm end}^2, \tag{5.1}$$

one obtains for the multipole moments ($l \geq 2$)

$$\langle a_l^2 \rangle = \frac{4}{3}\pi^2 \frac{(l+2)!}{(l-2)!} \frac{\rho_{\rm dS}}{\rho_P} \int_0^\infty \frac{d\kappa}{\kappa^{5/2}} \left\{ {}^1\tau_2^1(x_1,\kappa) G_l^2(\kappa) - {}^2\tau_2^1(x_1,\kappa) G_l^1(\kappa) \right\}^2 + O(\xi^1). \tag{5.2}$$

The integral above is simply an integral over the (rescaled, dimensionless) wave number κ, and again, strictly speaking, is ultraviolet divergent and should be cut off at some large $\kappa_{\rm max}$ (see Appendix C). The functions ${}^j\tau_2^1(x_1,\kappa)$ are the same functions defined in (A20). The functions $G_l^j(\kappa)$ are the (reparametrized) Sachs-Wolfe integrals over null geodesics, given by

$$G_l^j(\kappa) \equiv \int_{x_{\rm LS}}^{x_0} dx \frac{J_{l+1/2}(2\kappa^{1/2}(x_0 - x))}{(x_0 - x)^{5/2}(x^2-1)^{1/2}} \left\{ \frac{x}{x^2-1} {}^j\Sigma_2^1(x,\kappa) - {}^j\Sigma_2^{1\prime}(x,\kappa) \right\}, \tag{5.3}$$

where the limits $x_{\rm LS}$ and x_0 on the integral are given in terms of redshift by

$$x_0 \equiv \sqrt{2 + Z_{\rm eq}} \quad \text{and} \quad x_{\rm LS} \equiv \sqrt{1 + \frac{1+Z_{\rm eq}}{1+Z_{\rm LS}}}. \tag{5.4}$$

These formulas, and especially the spheroidal wave functions, may be numerically evaluated using the techniques discussed in Appendix B. Henceforth we refer to (5.2) and (5.3) as the "mixed" formulas for the multipole moments. Furthermore, we refer to multipole moments calculated using (5.2) and (5.3) as the "mixed" multipoles.

B. Numerical results

We have numerically evaluated the "mixed" formulas (5.2) and (5.3). The second column of Table II shows the "mixed" multipoles. The third column of Table II shows the results obtained by evaluating Eq. (6.2) of Allen and Koranda [2], which we refer to as the "exact-dust" formula for the multipole moments. The "exact-dust" formula assumes (1) the universe begins with an initial de Sitter phase, followed by (2) a pure radiation phase containing only radiation and no dust, followed by (3) a pure dust phase containing only dust and no radiation, during which (4) last scattering takes place. We refer to this type of universe as a "dust" universe, to distinguish it from the model described by (3.9), (3.11), and (3.15), which we refer to as a "mixed" universe because it contains both dust and radiation at and after last scattering. The fourth column shows the results obtained by evaluating Eq. (6.1) of Allen and Koranda, which we refer to as the "approximate-dust" formula for the multipole moments. The "approximate-dust" formula is a long-wavelength approximation to the "exact-dust" formula, and is *equivalent* to the standard formulas for the multipole moments given by Abbott and Wise [5] and Starobinsky [6]. The fifth column shows recent results of Ng and Speliotopoulos [10], who numerically integrated the wave equation to obtain the amplitude of the gravitational wave (or graviton mode function). They also

TABLE II. Multipole moments $\langle a_l^2 \rangle$ evaluated using different methods. These have been divided by the scale of the moments ρ_{DS}/ρ_P. The second column shows multipoles for a mixed cosmology obtained from the formulas (5.2) and (5.3), which analytically model a universe containing both dust and radiation, and which is not completely dust dominated at last scattering. The third column shows results obtained by evaluating Eq. (6.2) of Allen and Koranda [2], which assumes that the universe was completely dust dominated at last scattering. The fourth column shows results obtained by evaluating Eq. (6.1) of Allen and Koranda, which is a long-wavelength approximation to their Eq. (6.2), and equivalent to standard formula of Abbott and Wise [5] and Starobinsky [6]. The fifth column shows results obtained by Ng and Speliotopoulos [10], who numerically integrated the wave equation to obtain the amplitude of the gravitational waves. They also considered a universe model which is not completely dust dominated at last scattering. All the results were obtained with $Z_{eq} = 6000$ and $Z_{1S} = 1100$.

l	$\langle a_l^2 \rangle \frac{\rho_P}{\rho_{DS}}$ This work Eq. (5.2)	$\langle a_l^2 \rangle \frac{\rho_P}{\rho_{DS}}$ Allen, Koranda Eq. (6.2) of Ref. [2]	$\langle a_l^2 \rangle \frac{\rho_P}{\rho_{DS}}$ Allen, Koranda Eq. (6.1) of Ref. [2]	$\langle a_l^2 \rangle \frac{\rho_P}{\rho_{DS}}$ Ng, Speliotopoulos Table 1 of Ref. [10]
2	1.55	1.52	1.52	1.55
3	6.10×10^{-1}	6.07×10^{-1}	6.07×10^{-1}	
4	3.46×10^{-1}	3.44×10^{-1}	3.44×10^{-1}	
5	2.28×10^{-1}	2.27×10^{-1}	2.27×10^{-1}	
6	1.64×10^{-1}	1.62×10^{-1}	1.62×10^{-1}	
7	1.24×10^{-1}	1.22×10^{-1}	1.22×10^{-1}	
8	9.70×10^{-2}	9.61×10^{-2}	9.58×10^{-2}	
9	7.84×10^{-2}	7.74×10^{-2}	7.71×10^{-2}	
10	6.46×10^{-2}	6.37×10^{-2}	6.34×10^{-2}	
20	1.75×10^{-2}	1.69×10^{-2}	1.66×10^{-2}	1.75×10^{-2}
50	2.36×10^{-3}	1.99×10^{-3}	1.83×10^{-3}	2.36×10^{-3}
100	1.91×10^{-4}	8.67×10^{-5}	6.23×10^{-5}	1.90×10^{-4}
150	7.46×10^{-6}	4.11×10^{-6}	1.89×10^{-6}	7.41×10^{-6}
200	4.56×10^{-6}	3.68×10^{-6}	9.96×10^{-7}	4.49×10^{-6}

considered a universe model which contains both radiation and dust at last scattering. All of the results in Table II were obtained with $Z_{eq} = 6000$ and $Z_{LS} = 1100$.

Figures 1, 2, and 3 compare the "mixed" multipole moments to the multipole moments calculated using other techniques. The quantity M_l in Figs. 1–3 is defined by

$$M_l \equiv \frac{l(l+1)}{6}\frac{\langle a_l^2 \rangle}{\langle a_2^2 \rangle}. \tag{5.5}$$

(Note that in Ref. [2] the equation defining M_l in the caption of Fig. 2 contains an extraneous factor of ρ_{DS}/ρ_P.) Figure 1 compares multipoles calculated using the "mixed" or analytic formulas (5.2) and (5.3) to results from Turner, White, and Lidsey (TWL) [9]. TWL express the multipole moments in terms of the standard long-wavelength approximate mode functions [2] using a "transfer function." Figure 2 compares multipoles calculated using the "mixed" or dust and radiation analytic formulas to multipoles calculated using the Abbott and Wise [5] and Starobinsky [6] or "approximate-dust" formula. Figure 3 compares the "mixed" multipoles to the results of Crittenden *et al.* [11], who do not (directly) use the Sachs-Wolfe formula to calculate the CBR anisotropy. Instead they use numerical methods to evolve the photon distribution function using first-order perturbation theory of the general relativistic Boltzmann equation for radiative transfer. All the multipole moments shown in Figs. 1, 2, and 3 are for cosmological parameters

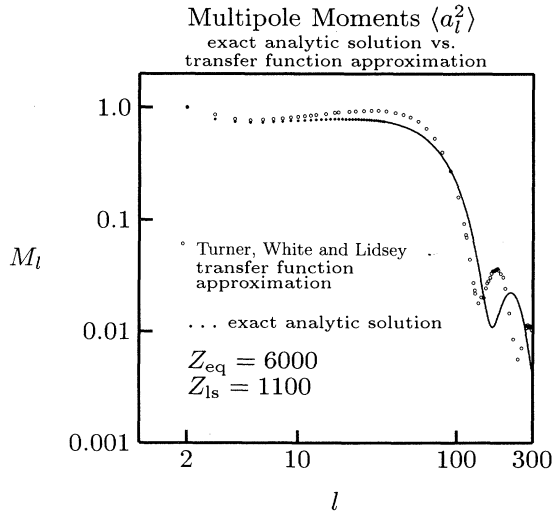

FIG. 1. Multipole moments $\langle a_l^2 \rangle$ normalized to the quadrupole $\langle a_2^2 \rangle$. The horizontal axis is the index l of the multipole moment and the vertical axis is M_l. See (5.5) for the definition of M_l. The points labeled "exact analytic solution" show results obtained from (5.2) and (5.3) which analytically model a universe containing both dust and radiation, and which is not completely dust dominated at last scattering. The points labeled "Turner, White and Lidsey transfer function approximation" show results from Turner, White, and Lidsey [9] obtained using a transfer function.

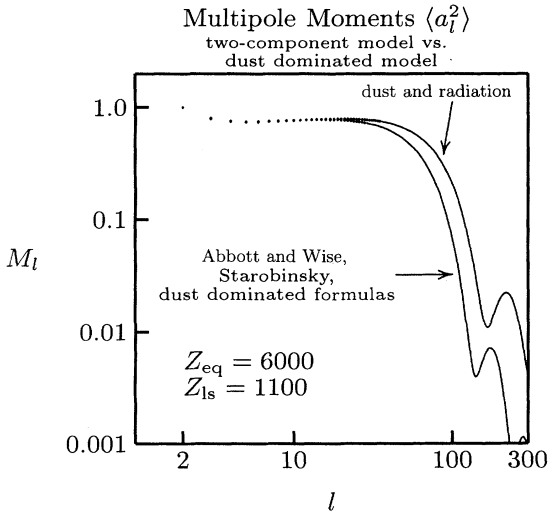

FIG. 2. Multipole moments $\langle a_l^2 \rangle$ normalized to the quadrupole $\langle a_2^2 \rangle$. The axes are the same as in Fig. 1. The points labeled "dust and radiation" show results obtained from (5.2) and (5.3) which analytically model a universe containing both dust and radiation, and which is not completely dust dominated at last scattering. The points labeled "Abbott and Wise, Starobinsky, dust dominated formulas" show results obtained using Eq. (6.1) of Allen and Koranda [2] [which is a long-wavelength approximation to Eq. (6.2) of Allen and Koranda [2]], which assumes that the universe is *completely* dust dominated at last scattering.

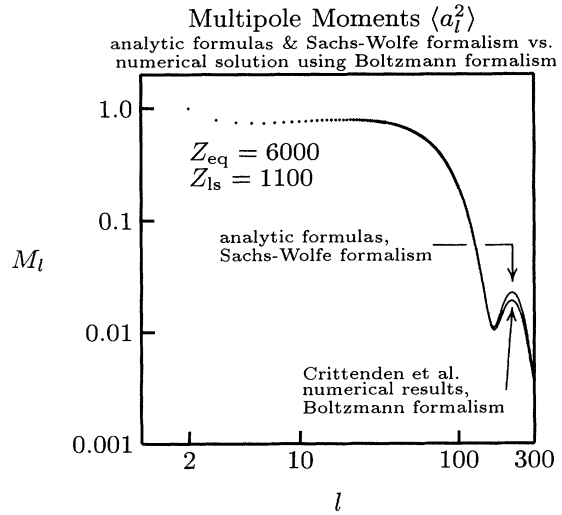

FIG. 3. Multipole moments $\langle a_l^2 \rangle$ normalized to the quadrupole $\langle a_2^2 \rangle$. The axes are the same as in Fig. 1. The points labeled "analytic formulas, Sachs-Wolfe formalism" show results obtained from (5.2) and (5.3) which analytically model a universe containing both dust and radiation, and which is not completely dust dominated at last scattering. The points labeled "Crittenden *et al.* numerical results, Boltzmann formalism" show results from Crittenden *et al.* [11], who do not use the Sachs-Wolfe formula (directly) to calculate the CBR anisotropy. Instead they use numerical methods to evolve the photon distribution function using first-order perturbation theory of the general relativistic Boltzmann equation for radiative transfer.

$Z_{eq} \approx 6000$ and $Z_{LS} = 1100$. (The values of Z_{eq} for the Turner-White-Lidsey work and for the results of Crittenden *et al.* differ from 6000 by about 1%.)

C. Discussion

The Ng-Speliotopoulos multipoles agree quite well with the "mixed" multipoles obtained here, using spheroidal wave functions, for a cosmology containing dust and radiation components. This is expected because the two methods used to calculate the multipole moments should be essentially equivalent. The graviton mode functions Ng and Speliotopoulos obtain by numerically integrating the wave equation (with the correct boundary conditions) must be equivalent to our analytic expressions (4.18). The cosmological model Ng and Speliotopoulos consider, however, is slightly different than our own. They model the smooth transition during the mixed phase by a simpler scale factor than our own (3.9). This may account for the small discrepancy between their results and our own.

The multipoles of Crittenden *et al.* (Fig. 3) also agree quite well with the "mixed" multipoles. This is also expected since the Boltzmann formalism [11,12] and the Sachs-Wolfe formalism should yield equivalent results. The discrepancy between the "mixed" multipoles and the multipoles of Crittenden *et al.* for $170 \lesssim l \lesssim 270$ is most likely due to our idealized treatment of the last scattering event [24,25]. In our analysis the last scattering is an *instantaneous* event occurring at redshift $Z_{LS} = 1100$. The analysis of Crittenden *et al.* [11] is more physically realistic. In their analysis the last scattering event is a dynamic process that takes place over a range of redshift $1000 \lesssim Z_{LS} \lesssim 1200$ [25]. This more realistic treatment of the last scattering event has the effect of "washing out" the smaller angle anisotropy and thus decreasing the higher l multipoles. In future work we modify our analysis to treat the last scattering in a more physical way [26].

For $l \lesssim 30$, the "approximate-dust" multipoles agree fairly well with the "mixed" multipoles (Fig. 2). This is not surprising. The small l multipoles $\langle a_l^2 \rangle$ are most affected by longer-wavelength perturbations. These longer-wavelength perturbations were redshifted outside the Hubble sphere early in the inflationary phase, and only recently reentered the Hubble sphere (the longest-wavelength perturbations remain outside the Hubble sphere even today [22]). Because they remained outside the Hubble sphere until recently, the longer-wavelength perturbations are insensitive to the details of the evolution of the universe before it became dust dominated. Thus, the "mixed" universe and "dust" universe models are essentially equivalent for longer-wavelength perturbations. So it is not surprising that the same CBR anisotropies are produced by the long-wavelength perturbations in either model. Thus the "approximate-dust" and "mixed" multipoles should, and do, agree for small l. Furthermore, because the "approximate-dust" formula for the multipole moments is equivalent to the standard formulas given by Abbott and Wise [5] and Starobinsky

[6], one can conclude that the standard formulas for the multipole moments are accurate for small l, whether or not the universe was completely dust dominated at last scattering.

For $l \gtrsim 30$, the "approximate-dust" multipoles differ significantly from the "mixed" multipoles. Again this is not surprising. The larger l multipoles are more affected by shorter-wavelength perturbations, which reentered the Hubble sphere before the universe became dust dominated, and are therefore sensitive to the details of the cosmological expansion before dust domination. A "mixed" universe becomes dust dominated *much more slowly* than a "dust" universe, which is dust dominated immediately after the radiation phase ends at dust-radiation equality $\eta_{\rm eq}$. Therefore the shorter-wavelength modes in a "mixed" universe and a "dust" universe evolve very differently after they reenter the Hubble sphere. This difference is evident in Fig. 2 for the large l multipole moments.

The TWL multipole spectrum differs significantly from the "mixed" multipole spectrum (Fig. 1). In particular their multipole moments are significantly greater than the "mixed" multipoles for $3 \lesssim l \lesssim 80$. Although TWL consider a "mixed" universe, they use the standard multipole moment formulas for a "dust" universe. However, they modify the standard formulas by including a time-independent transfer function $T(k/k_{\rm eq})$, which depends only on the wave number k [see Eqs. (22), (23) of Ref. [9]]. TWL give an explicit functional form for the transfer function [Eq. (15) of Ref. [9]], which they obtain by numerically integrating the wave equation [9]:

$$T(y) = [1.0 + 1.34y + 2.50y^2]^{1/2} \quad \text{where } y = k/k_{\rm eq}. \quad (5.6)$$

Since the transfer function $T \geq 1$ appears in the expression for the multipole moments as $|T(k/k_{\rm eq})|^2$ [see Eqs. (22), (23) of [9]], one can see that the effect of the transfer function (5.6) is to *increase* the multipole moments. Furthermore, the contribution from shorter-wavelength (larger k) modes is enhanced more than the contribution from longer-wavelength (smaller k) modes, since $T(k/k_{\rm eq}) \to 1$ as $k \to 0$.

Since the TWL multipoles are significantly greater than the "mixed" multipoles for $3 \lesssim l \lesssim 80$, *the transfer function overestimates the contribution to the multipole moments from longer-wavelength modes.* This is easy to see. As discussed above, the standard formulas are accurate for small l multipoles, and give essentially the same results as the "mixed" formulas for $l \lesssim 30$. The TWL formulas for the multipole moments are equivalent to the standard formulas, except for the transfer function. Thus, if the transfer function was set to unity, the TWL multipoles would be the same as the standard multipoles, and hence would be equivalent to the "mixed" multipoles for $l \lesssim 30$. Since the TWL multipoles are larger than the "mixed" multipoles for $3 \lesssim l \lesssim 80$, the transfer function must enhance the the contribution to the $3 \lesssim l \lesssim 80$ multipole moments too much. Because the small l moments are affected most by longer-wavelength perturbations, the transfer function must overestimate the contribution from longer wavelengths or smaller wave number k.

The TWL multipole spectrum is also significantly different than the "mixed" multipole spectrum for large l. The large l multipoles are most affected by shorter-wavelength modes. The transfer function (5.6) significantly enhances the contribution of shorter-wavelength modes (larger k) to the multipole moments. Because the TWL transfer function (5.6) is time independent, however, it cannot alter the time evolution of the shorter-wavelength modes. By comparing the "dust" universe graviton mode function [see Eq. (4.28) of [2]]

$$\phi(\eta, k)_{\rm dust} = \sqrt{\frac{24}{\pi}\frac{\rho_{\rm dS}}{\rho_P}}\frac{j_1\Big(k(\eta+\eta_{\rm eq})\Big)}{k^{5/2}(\eta+\eta_{\rm eq})} \quad (5.7)$$

(which is equivalent to the standard formulas for the gravity-wave amplitude [2], and hence equivalent to the TWL formulas for the gravity-wave amplitude) to the "mixed" universe mode function (4.18), one can see that the time evolution of the shorter-wavelength modes is very different in a "dust" universe when compared to the time evolution in a "mixed" universe. In their paper (at the end of Sec. II D), TWL discuss the accuracy of their transfer function approximation. They conclude that neglecting the redshift dependence (i.e., time dependence) of the transfer function and "pulling it out" of the Sachs-Wolfe integral results in a maximum error of about 20% if the universe contains significant amounts of radiation at last scattering. We agree with the 20% bound on the TWL error, and agree that this is the source of the discrepancy between our results. The results of our analytic calculation are more accurate because we do not make the approximation made in the TWL work.

VI. CONCLUSION

This paper examines the tensor perturbations of the gravitational field in a spatially flat, FRW cosmology containing a mixture of radiation and dust, and shows that they may be expressed in terms of spheroidal wave functions. Although spheroidal wave functions have appeared in this context before, previous authors incorrectly determined the characteristic exponent which parametrizes these functions. After explaining the correct method for determining the characteristic exponent, we show that spheroidal wave functions may be efficiently and accurately evaluated using standard numerical techniques.

We considered inflationary cosmological models, and used the spheroidal wave functions to find the spectrum of CBR temperature fluctuations resulting from primordial tensor (gravitational radiation) perturbations. These temperature fluctuations are predicted by all inflationary models. Their existence follows from first principles: It is a consequence of the uncertainty principle and the Einstein equation. The temperature fluctuations have been previously studied by a number of authors (including ourselves) using a variety of approximations, and both analytic and numerical techniques.

In hindsight, only three approximations remain in this work. One is that the amplitude of the gravitational perturbation h_{ij} is very small. This approximation is indeed well justified. The second approximation is that the energy density and pressure of the universe correspond to a mixture of dust and radiation as given in (3.11)–(3.15). Going back in time, this approximation is good until approximately the time of nucleosynthesis, $t = 200$ sec, when the number of effectively massless particles in the universe changed. This should not affect the multipole moments $\langle a_l^2 \rangle$ which we consider, which have $l < 300$. The final approximation, that the last scattering surface is very thin, is currently under investigation [26].

It is likely that the spheroidal wave functions, which describe gravitational wave perturbations in realistic cosmological models, will find other useful applications. We expect that the results and methods of this paper may prove applicable to a wider variety of calculations than the CBR temperatures perturbations considered here.

ACKNOWLEDGMENTS

We are grateful to Rob Caldwell, Scott Dodelson, Edward Kolb, Lloyd Knox, Jorma Louko, Mike Turner, and Martin White for useful comments and suggestions. We thank Paul Steinhardt for providing the multipoles of Crittenden *et al.* shown in Fig. 3. This work has been partially supported by NSF Grant No. PHY91-05935.

APPENDIX A

In spatially flat FRW universes, graviton mode functions in a linearized theory of gravity obey a minimally coupled, massless, scalar wave equation [27] like (2.5). If the scale factor of the spatially flat FRW universe transforms smoothly from being radiation to dust dominated, the solutions to the equation are spheroidal wave functions.

1. Differential equation of spheroidal wave functions and its solutions

There is no generally accepted "standard" form for the differential equation of spheroidal wave functions. We write the differential equation as

$$\frac{d^2\varphi}{dz^2} - \frac{2z}{(1-z^2)}\frac{d\varphi}{dz} + \left\{ \frac{\lambda}{(1-z^2)} + 4\theta - \frac{\mu^2}{(1-z^2)^2} \right\}\varphi = 0. \quad \text{(A1)}$$

The parameters μ, λ, and θ and the variable z can in general be complex. Here we take z, λ, μ, and θ to be real. We also consider only $\theta \geq 0$. The differential equation (A1) has two regular singular points at $z = \pm 1$ and an irregular singular point at $z = \infty$. We only consider $z > 1$. Then the solutions of (A1) are the *spheroidal wave functions* [28,29]

$$\varphi = S_\nu^{\mu(j)}(z,\theta), \quad z > 1, \quad j = 1,2,3,4. \quad \text{(A2)}$$

The parameter μ is the *order* of the spheroidal wave function, and ν is the *characteristic exponent.* In later sections we consider in detail the characteristic exponent ν and its relation to the order μ and the parameters λ and θ. For now we simply note that ν is restricted so that

$$\nu + 1/2 \neq \text{ integer}. \quad \text{(A3)}$$

For a very thorough and complete discussion of the differential equation (A1) and the solutions (A2) see Ref. [29].

The spheroidal wave functions can be expressed in terms of more familiar special functions. If $\theta = 0$, then the differential equation (A1) reduces to Legendre's differential equation, suggesting that the spheroidal wave functions can be expressed in terms of Legendre functions [28,29]. For $z > 1$, however, it is more useful to express the spheroidal wave functions as infinite sums of Bessel functions. For $\mu > 0$ one can write the spheroidal functions as

$$S_\nu^{\mu(j)}(z,\theta) = \left(\frac{z^2}{z^2-1}\right)^{\mu/2} T_\nu^{\mu(j)}(z,\theta), \quad \mu > 0, \quad \text{(A4)}$$

where $T_\nu^{\mu(j)}(z,\theta)$ is the infinite sum

$$T_\nu^{\mu(j)}(z,\theta) = s_\nu^\mu(\theta) \sum_{r=-\infty}^{\infty} a_{\nu,r}^\mu(\theta)\psi_{\nu+2r}^{(j)}(2\theta^{1/2}z), \quad j = 1,2,3,4. \quad \text{(A5)}$$

The expansion coefficients $a_{\nu,r}^\mu(\theta)$ and the normalization factor $s_\nu^\mu(\theta)$, which are the same for any j, are discussed below. The functions $\psi_\upsilon^{(j)}(z)$ are proportional to Bessel or Hankel functions

$$\begin{aligned} \psi_\upsilon^{(1)}(z) &= \sqrt{\tfrac{\pi}{2z}} J_{\upsilon+1/2}(z), \\ \psi_\upsilon^{(2)}(z) &= \sqrt{\tfrac{\pi}{2z}} Y_{\upsilon+1/2}(z), \\ \psi_\upsilon^{(3)}(z) &= \sqrt{\tfrac{\pi}{2z}} H_{\upsilon+1/2}^{(1)}(z), \\ \psi_\upsilon^{(4)}(z) &= \sqrt{\tfrac{\pi}{2z}} H_{\upsilon+1/2}^{(2)}(z). \end{aligned} \quad \text{(A6)}$$

The spheroidal wave function of the first kind ($j = 1$) and the spheroidal wave function of the second kind ($j = 2$) form a complete solution to the differential equation (A1). Because the Hankel functions $H_\upsilon^{(1)}(z) = J_\upsilon(z) \pm iY_\upsilon(z)$ can be written as linear combinations of Bessel functions (see Eq. (3.86) in Ref. [21]), the spheroidal functions of the third ($j = 3$) and fourth ($j = 4$) kind can be written as linear combinations of spheroidal functions of the first and second kinds:

$$\begin{aligned} S_\nu^{\mu(3)}(z,\theta) &= S_\nu^{\mu(1)}(z,\theta) + iS_\nu^{\mu(2)}(z,\theta), \\ S_\nu^{\mu(4)}(z,\theta) &= S_\nu^{\mu(1)}(z,\theta) - iS_\nu^{\mu(2)}(z,\theta). \end{aligned} \quad \text{(A7)}$$

The spheroidal functions of the third and fourth kinds also form a complete solution to the spheroidal differential equation. The expansions (A4) of the spheroidal wave functions in terms of Bessel and Hankel functions are only useful if the infinite sums (A5) converge.

The convergence of the infinite sums depends on the expansion coefficients $a^{\mu}_{\nu,r}(\theta)$. Substituting (A4) and (A5) into the differential equation (A1) yields a three-term recurrence relation that the expansion coefficients must satisfy. The recurrence relation can be written as

$$\mathcal{A}^{\mu}_{\nu,r}(\theta)a^{\mu}_{\nu,r-1}(\theta)+\mathcal{B}^{\mu}_{\nu,r}(\theta)a^{\mu}_{\nu,r}(\theta)+\mathcal{C}^{\mu}_{\nu,r}(\theta)a^{\mu}_{\nu,r+1}(\theta)=0, \tag{A8}$$

where

$$\begin{aligned}\mathcal{A}^{\mu}_{\nu,r}(\theta)&=4\theta\frac{(\nu+2r-\mu)(\nu+2r-\mu-1)}{(2\nu+4r-3)(2\nu+4r-1)},\\ \mathcal{B}^{\mu}_{\nu,r}(\theta)&=\lambda-(\nu+2r)(\nu+2r+1)\\ &\quad+\frac{(\nu+2r)(\nu+2r+1)+\mu^2-1}{(2\nu+4r-1)(2\nu+4r+3)}8\theta,\\ \mathcal{C}^{\mu}_{\nu,r}(\theta)&=4\theta\frac{(\nu+2r+\mu+2)(\nu+2r+\mu+1)}{(2\nu+4r+3)(2\nu+4r+5)}.\end{aligned} \tag{A9}$$

The solution to this recurrence relation, as well as the convergence of the infinite sums (A5), depends critically on the parameters μ, ν, λ, and θ, and is discussed below. Once a solution to the recurrence relation [for which the infinite sums (A5) converge] is obtained, the normalization factor $s^{\mu}_{\nu}(\theta)$ is given by

$$s^{\mu}_{\nu}(\theta)=\left[\sum_{r=-\infty}^{\infty}(-1)^r a^{\mu}_{\nu,r}(\theta)\right]^{-1}. \tag{A10}$$

This normalization is chosen so that in the limit as z becomes very large:

$$\lim_{z\to\infty}\left[S^{\mu(j)}_{\nu}(z,\theta)/\psi^{(j)}_{\nu}(2\theta^{1/2}z)\right]=1. \tag{A11}$$

This relation and many more details of the solutions (A4) are developed in Ref. [29].

2. Eigenvalue λ

Although the order μ of the spheroidal wave function, along with the parameters θ and λ, appears directly in the differential equation (A1), the characteristic exponent ν does not. In most investigations and applications of spheroidal wave functions [28–31], however, the parameter λ is left unfixed; one *assumes* a (typically integer) value for ν and considers λ to be a function of μ, ν, and θ and writes

$$\lambda=\lambda^{\mu}_{\nu}(\theta). \tag{A12}$$

$\lambda^{\mu}_{\nu}(\theta)$ is often referred to as an eigenvalue, especially when considering spheroidal wave functions as solutions to the three-dimensional wave equation [32].

For a given choice of the parameters μ, ν, and θ, the eigenvalue $\lambda^{\mu}_{\nu}(\theta)$ is that value of λ for which the recurrence relation (A8) has a *minimal* solution. A minimal solution, roughly speaking, is a set of coefficients $a^{\mu}_{\nu,r}(\theta)$ that satisfy the recurrence relation *and* fall off for large $|r|$ [33]. A *dominant* solution is a set of coefficients that satisfy the recurrence relation but do not fall off. If the solution to the recurrence relation is a dominant solution, the coefficients $a^{\mu}_{\nu,r}(\theta)$ do not fall off for large $|r|$, and the infinite sums in (A5) may not converge. In general a three-term recurrence relation will have two independent solutions, much like a second-order, ordinary differential equation. However, neither of the two solutions, nor any linear combination of the two solutions, need be a minimal solution [33]. For a given set of parameters μ, ν, and θ, a minimal solution to the recurrence relation (A8) exists only for a single, discrete value of λ. That value for which the minimal solution exists is the eigenvalue $\lambda^{\mu}_{\nu}(\theta)$. In our problem, we are given λ, θ, and μ. One can find ν (modulo an integer) by requiring that the recurrence relation (A8) have a minimal solution; i.e., ν is determined, modulo an integer, by the requirement that (A8) have a minimal solution.

The functional relationship between the parameters μ,ν,θ and the eigenvalue $\lambda^{\mu}_{\nu}(\theta)$ is complicated. It has been shown [28] that the functional relationship can be expressed as

$$\cos(2\pi\nu)=f(\lambda,\mu^2,\theta), \tag{A13}$$

where a closed, analytic form for the function f is usually unattainable. The relation (A13) only determines the characteristic exponent ν (as a function of λ, μ, and θ) up to an integer; a second constraint [29] fixes ν:

$$\lambda^{\mu}_{\nu}(\theta=0)=\nu(\nu+1). \tag{A14}$$

In Sec. IV B the special case of the differential equation (A1) with $\lambda=2$ is considered. The constraint (A14), along with the condition (A3) that ν not be a half-integer, fixes ν so that

$$\frac{1}{2}<\nu<\frac{3}{2}\ \text{for}\ \lambda=2. \tag{A15}$$

For investigations of some of the analytic properties of $f(\lambda,\mu^2,\theta)$ see Ref. [29]. A more practical method for finding the functional relation between the parameters μ, ν, θ, and λ is discussed in Appendix A 6 below.

3. Case $\mu=1$, $\lambda=2$

The special case of the differential equation (A1) with $\mu=1$ and $\lambda=2$ is of cosmological interest, and has been previously studied by Sahni [19] and Nariai [20], who incorrectly take the solution to be $S^{1(4)}_{1}$. In spatially flat FRW universes containing a mixture of dust and radiation, one may cast the wave equation for graviton mode functions in the form of the spheroidal wave function differential equation, as shown in Sec. IV B. The differential equation the graviton mode function obeys, (4.14),

is the special case of the differential equation (A1) with $\mu = 1$, $\lambda = 2$, and θ arbitrary. (θ is arbitrary since in Sec. IV B it is proportional to the wave number of a graviton mode function, and we desire expressions for the mode functions that are valid for an interesting range of wave numbers.) Even if one takes λ in (A1) to be fixed and does not consider the eigenvalue problem for λ, the arguments and conclusion in the previous paragraph are still valid, especially the constraint (A13); if μ, ν, λ, and θ do not satisfy (A13), a minimal solution to the recurrence relation does not exist and the infinite sums in (A5) do not converge. If $\lambda = 2$, $\mu = 1$, and θ is arbitrary, then the characteristic exponent ν is determined by the constraint (A13) with $\lambda = 2$ and $\mu = 1$. Tables of eigenvalues $\lambda^{\mu}_{\nu}(\theta)$ for different values of μ, ν, and θ have been published [31], however, and from these one can determine that the solution to (A13) for $\mu = 1$, $\lambda = 2$, and θ arbitrary is *not* $\nu = 1$: i.e.,

$$\cos(2\pi) \neq f(2, 1, \theta) \text{ for arbitrary } \theta. \tag{A16}$$

So for arbitrary θ the solution to the differential equation (A1) with $\mu = 1$ and $\lambda = 2$ is *not* the spheroidal wave function (A2) with $\mu = 1$ and $\nu = 1$: i.e.,

$$\varphi \neq S_1^{1(j)}(z, \theta) \text{ for } \lambda = 2. \tag{A17}$$

This subtle point is missed in [19,20], where the solution to the spheroidal wave function differential equation with $\mu = 1$, $\lambda = 2$, and θ arbitrary is incorrectly given as $S_1^{1(4)}$.

4. More suitable notation

The notation introduced above for the spheroidal wave functions (A2) is most useful when the order μ and the characteristic exponent ν are fixed, and the eigenvalue $\lambda^{\mu}_{\nu}(\theta)$ is considered as a function of μ, ν, and θ. Since we are most interested in the case when μ and λ are fixed, it is more descriptive to denote the characteristic exponent as $\nu = \nu^{\mu}_{\lambda}(\theta)$. This convention, however, would have one denote the spheroidal wave functions as $S^{\mu(j)}_{\nu^{\mu}_{\lambda}(\theta)}(z, \theta)$, which is cluttered and inconvenient. In Sec. IV B, where θ is itself a function (of wave number), the notation would be even more unpleasant.

For this reason we adopt a new notation for the spheroidal wave functions. The solution to the differential equation (A1) with μ and λ fixed is denoted

$${}^{j}\Sigma^{\mu}_{\lambda}(z, \theta) \equiv S^{\mu(j)}_{\nu^{\mu}_{\lambda}(\theta)}(z, \theta). \tag{A18}$$

The function on the left-hand side above is, of course, the same function as on the right-hand side, expressed using a different notation. *The lower index on the left-hand side above is the "eigenvalue" λ ($\lambda \equiv 2$ for the cosmological problem) and not the characteristic exponent ν.* The upper index μ is again the order of the spheroidal wave function, and again the index $j = 1, 2, 3, 4$ labels the four solutions. In terms of Bessel functions, the spheroidal wave function is now written as

$${}^{j}\Sigma^{\mu}_{\lambda}(z, \theta) = \left(\frac{z^2}{z^2 - 1}\right)^{\mu/2} {}^{j}\tau^{\mu}_{\lambda}(z, \theta), \tag{A19}$$

where

$${}^{j}\tau^{\mu}_{\lambda}(z, \theta) \equiv s^{\mu}_{\lambda}(\theta) \sum_{r=-\infty}^{\infty} a^{\mu}_{\lambda, r}(\theta) \psi^{(j)}_{\nu+2r}(2\theta^{1/2} z), \tag{A20}$$

with $\nu = \nu^{\mu}_{\lambda}(\theta)$, and the $\psi^{(j)}_{\upsilon}$ are the same functions given in (A6). The expansion coefficients $a^{\mu}_{\lambda}(\theta)$ are the same as those in (A5) and obey the same recurrence relation (A8) with the obvious change in notation. The normalization factor $s^{\mu}_{\lambda}(\theta)$ is also the same as in (A5) with the obvious change in notation. We use this notation in Secs. IV B, IV C, and V A, and the rest of this appendix.

5. Wronskian and complex conjugates

Two relations for the spheroidal wave functions are especially useful in Sec. IV B. The first involves the spheroidal wave functions of the third and fourth kinds, and is obvious from the relations (A7):

$${}^{4}\Sigma^{\mu}_{\lambda}(z, \theta) = \left[{}^{3}\Sigma^{\mu}_{\lambda}(z, \theta)\right]^{*}. \tag{A21}$$

Here an asterisk denotes complex conjugation. The second relation is the Wronskian for the spheroidal wave functions of the third and fourth kinds:

$$W\left[{}^{4}\Sigma^{\mu}_{\lambda}(z, \theta), {}^{3}\Sigma^{\mu}_{\lambda}(z, \theta)\right] \equiv {}^{4}\Sigma^{\mu}_{\lambda}(z, \theta) \frac{d}{dz} {}^{3}\Sigma^{\mu}_{\lambda}(z, \theta) - {}^{3}\Sigma^{\mu}_{\lambda}(z, \theta) \frac{d}{dz} {}^{4}\Sigma^{\mu}_{\lambda}(z, \theta) = \frac{i}{\theta^{1/2}(z^2 - 1)}. \tag{A22}$$

This relation, along with related results, is derived in Ref. [29] [see especially Sec. 3.65, Eq. (53)].

6. Practical method for determining $\nu^{\mu}_{\lambda}(\theta)$ and ${}^{j}\Sigma^{\mu}_{\lambda}(z, \theta)$

The constraints (A13) and (A14) determine $\nu^{\mu}_{\lambda}(\theta)$ for a given choice of μ, λ, and θ. In practice, however, it is difficult to use these constraints since a closed, analytic form for the function f is usually not known. Recall, though, that the constraint (A13) is equivalent to finding a minimal solution to the recurrence relation (A8). A minimal solution exists only for the single, discrete value of $\nu^{\mu}_{\lambda}(\theta)$ that satisfies the constraints (A13) and (A14).

One can use the theory of continued fractions to find the minimal solution to the recurrence relation and determine

$\nu^{\mu}_{\lambda}(\theta)$. Divide (A8) by $a_r(\theta)$ and consider the infinite continued fraction $P^{\mu}_{\lambda,r}(\theta)$ defined for $r \geq 1$ as

$$P^{\mu}_{\lambda,r}(\theta) \equiv \frac{a_r}{a_{r-1}} = \frac{-\mathcal{A}_r}{\mathcal{B}_r + \mathcal{C}_r \frac{a_{r+1}}{a_r}} = \cfrac{-\mathcal{A}_r}{\mathcal{B}_r + \mathcal{C}_r \cfrac{-\mathcal{A}_{r+1}}{\mathcal{B}_{r+1} + \mathcal{C}_{r+1} \cfrac{-\mathcal{A}_{r+2}}{\mathcal{B}_{r+2} + \cdots}}}} \quad r \geq 1, \tag{A23}$$

where we have again suppressed for clarity the indices μ and λ as well as the argument θ. For a given choice of parameters μ, λ, θ, and ν the infinite continued fraction can be used to find the ratios a_r/a_{r-1} of all the expansion coefficients, for $r \geq 1$, *if the continued fraction converges.* There is no loss of generality if one assumes $a_0 = 1$ [28,29] [note that this is compensated for in the normalization $s^{\mu}_{\lambda}(\theta)$], and so the continued fraction (if it converges) can be used to find the expansion coefficients a_r for $r \geq 1$.

A second infinite continued fraction for $r \leq -1$ can also be derived from the recurrence relation. We define the continued fraction

$$N^{\mu}_{\lambda,r}(\theta) \equiv \frac{a_r}{a_{r+1}} = \frac{-\mathcal{C}_r}{\mathcal{B}_r + \mathcal{A}_r \frac{a_{r-1}}{a_r}} = \cfrac{-\mathcal{C}_r}{\mathcal{B}_r + \mathcal{A}_r \cfrac{-\mathcal{C}_{r-1}}{\mathcal{B}_{r-1} + \mathcal{A}_{r-1} \cfrac{-\mathcal{C}_{r-2}}{\mathcal{B}_{r-2} + \cdots}}} \quad r \leq -1. \tag{A24}$$

Assuming $a_0 = 1$, the continued fraction (if it converges) can be used to find the expansion coefficients a_r for $r \leq -1$.

Whether or not the infinite continued fractions converge depends on the existence of minimal solutions to the recurrence relation. Pincherle's theorem [33] tells us that the infinite continued fraction $P^{\mu}_{\lambda}(\theta)$ converges for $r \geq 1$ if and only if the recurrence relation has a *minimal* solution for $r \geq 1$. Further, if the infinite continued fraction does converge, it converges to a minimal solution. Likewise, $N^{\mu}_{\lambda}(\theta)$ converges to a minimal solution for $r \leq -1$ if and only if the recurrence relation has a minimal solution for $r \leq -1$.

A subtle, but important, point is that $P^{\mu}_{\lambda}(\theta)$ and $N^{\mu}_{\lambda}(\theta)$ may converge *to different minimal solutions.* Given a set of parameters μ, λ, θ, and ν, the continued fraction (A23) (with $a_0 = 1$) may converge and determine a set of coefficients $a_1, a_2, a_3, \ldots$. These coefficients will satisfy the recurrence relation for $r \geq 1$ and will fall off for large r. Likewise, for the same set of parameters, the continued fraction (A24) may converge and determine a set of coefficients $a_{-1}, a_{-2}, a_{-3}, \ldots$, which will satisfy the recurrence relation for $r \leq -1$ and will fall off for large $|r|$. The recurrence relation for $r = 0$, however, *may not be satisfied.* This is because the $r = 0$ recurrence relation

$$\mathcal{A}^{\mu}_{\lambda,0}(\theta) a^{\mu}_{\lambda,-1}(\theta) + \mathcal{B}^{\mu}_{\lambda,0}(\theta) a^{\mu}_{\lambda,0}(\theta) + \mathcal{C}^{\mu}_{\lambda,0}(\theta) a^{\mu}_{\lambda,1}(\theta) = 0 \tag{A25}$$

is not explicitly solved when calculating either the $P^{\mu}_{\lambda}(\theta)$ or the $N^{\mu}_{\lambda}(\theta)$. One can see this by examining the continued fractions (A23) and (A24); the three coefficients a_{-1}, a_0, and a_1 do not appear together anywhere in (A23) and (A24) for any r. So both the set of expansion coefficients $a_1, a_2, a_3, \ldots$ found using $P^{\mu}_{\lambda}(\theta)$ and the set $a_{-1}, a_{-2}, a_{-3}, \ldots$ found using $N^{\mu}_{\lambda}(\theta)$ are minimal solutions for a certain range of the index r, but not for all r.

In order for the recurrence relation (A8) to be satisfied it must be true for *all* r. To ensure this, one must match the two solutions found using the continued fractions. This is accomplished by requiring that

$$\mathcal{A}^{\mu}_{\lambda,0}(\theta) N^{\mu}_{\lambda,-1}(\theta) + \mathcal{B}^{\mu}_{\lambda,0}(\theta) + \mathcal{C}^{\mu}_{\lambda,0}(\theta) P^{\mu}_{\lambda,1}(\theta) \equiv Z^{\mu}_{\lambda}(\theta,\nu) = 0, \tag{A26}$$

which is just the requirement that the recurrence relation be satisfied for $r = 0$. So finding the minimal solution to the recurrence relation, and hence the characteristic exponent $\nu^{\mu}_{\lambda}(\theta)$, is equivalent to finding the root of the function $Z^{\mu}_{\lambda}(\theta,\nu)$ defined in (A26). Given a test value for $\nu^{\mu}_{\lambda}(\theta)$, one calculates the continued fractions $P^{\mu}_{\lambda,1}(\theta)$ and $N^{\mu}_{\lambda,-1}(\theta)$, and the rational functions $\mathcal{A}^{\mu}_{\lambda,0}$, $\mathcal{B}^{\mu}_{\lambda,0}$, and $\mathcal{C}^{\mu}_{\lambda,0}$, to find $Z^{\mu}_{\lambda}(\theta,\nu)$. If Z^{μ}_{λ} is not zero, one modifies the test value for $\nu^{\mu}_{\lambda}(\theta)$ using whichever root-finding algorithm one prefers.

In practice, this method for determining $\nu^{\mu}_{\lambda}(\theta)$ is efficient. Figure 4 shows the function $Z^1_2(\theta,\nu)$ (of interest for the cosmological case) for $\theta = 5$ and $\frac{1}{2} < \nu < \frac{3}{2}$. This plot is typical for θ in the range $10^{-4} \leq \theta \leq 10^4$;

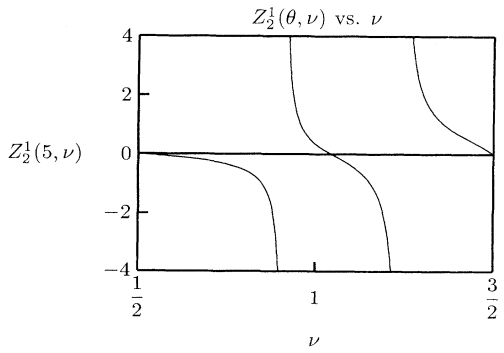

FIG. 4. The function $Z^1_2(\theta,\nu)$ plotted versus ν for $\theta = 5$. The value of ν at which this function vanishes is the characteristic exponent $\nu^1_2(\theta)$ for $\theta = 5$. This plot is typical for values of θ in the range $10^{-4} \leq \theta \leq 10^4$. The root is always located between two singularities.

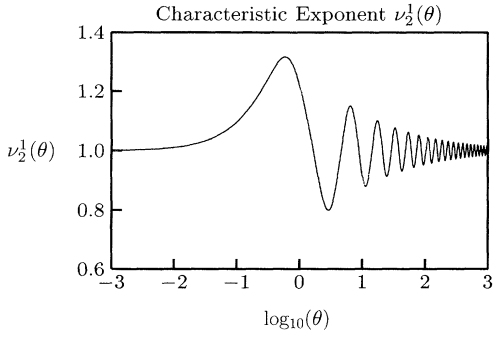

FIG. 5. The characteristic exponent $\nu_2^1(\theta)$ plotted vs $\log_{10}\theta$. Only for certain discrete values of θ is ν equal to 1. For this reason the function $S_1^{1(j)}(z,\theta)$ is not a valid solution to the differential equation (A1) for $\mu = 1, \lambda = 2$, and arbitrary θ.

the root $\nu_\lambda^\mu(\theta)$ is always located between two singularities, and Z_2^1 is positive for $\nu = \nu_\lambda^\mu(\theta) - \epsilon$ and negative for $\nu = \nu_\lambda^\mu(\theta) + \epsilon$ where $0 < \epsilon \ll 1$. This assists implementing a root-finding algorithm to find the zeros of $Z_2^1(\theta,\nu)$ for arbitrary θ. Figure 5 shows the characteristic exponent $\nu_2^1(\theta)$ for $10^{-3} \leq \theta \leq 10^3$.

Once the characteristic exponent $\nu_\lambda^\mu(\theta)$ is determined, one can use the continued fractions (A23) and (A24), along with $a_{\lambda,0}^\mu = 1$, to calculate the remaining expansion coefficients. Since these coefficients are the minimal solution, the coefficients fall off for large $|r|$. One can then use (A10) to find $s_\lambda^\mu(\theta)$. Using (A4) and (A5), along with an algorithm for computing Bessel and Hankel functions, one can evaluate the spheroidal wave functions. Further details of the numerical techniques used may be found in Appendix B. Figure 6 shows the spheroidal wave functions ${}^1\Sigma_2^1(z,\theta)$ and ${}^2\Sigma_2^1(z,\theta)$ as functions of z for two values of θ.

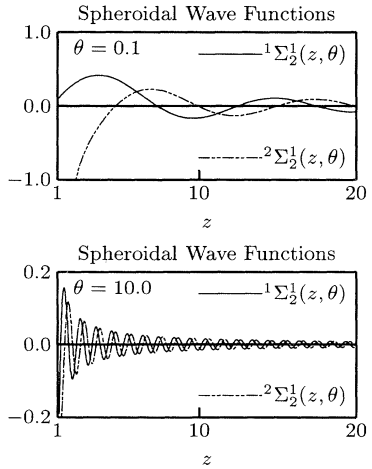

FIG. 6. The spheroidal wave functions ${}^1\Sigma_2^1(z,\theta)$ (solid lines) and ${}^2\Sigma_2^1(z,\theta)$ (dashed lines) for $\theta = 0.1$ and $\theta = 10$. Both functions diverge in the limit as $z \to 1$. Note that the vertical scales are different for the two plots.

APPENDIX B

This appendix briefly describes the numerical techniques used to obtain the results in Sec. V B. One may separate the problem of numerically evaluating the spheroidal wave functions ${}^1\Sigma_2^1(z,\theta)$ and ${}^2\Sigma_2^1(z,\theta)$ into two parts. The first is to determine the characteristic exponent $\nu_2^1(\theta)$ for a given θ. As noted in Appendix A 6 the characteristic exponent $\nu_2^1(\theta)$ is that value of ν for which the function $Z_2^1(\theta,\nu)$ vanishes, where

$$Z_2^1(\theta,\nu) \equiv \mathcal{A}_{2,0}^1(\theta) N_{2,-1}^1(\theta) + \mathcal{B}_{2,0}^1(\theta) + \mathcal{C}_{2,0}^1(\theta) P_{2,1}^1(\theta). \tag{B1}$$

To find the root of $Z_2^1(\theta,\nu)$ [and hence the characteristic exponent $\nu_2^1(\theta)$] one must evaluate the five functions on the right-hand side of (B1). From (A9) one can see that the three functions $\mathcal{A}_{2,0}^1$, $\mathcal{B}_{2,0}^1$, and $\mathcal{C}_{2,0}^1$ (here $\lambda = 2$, *not* ν) are rational functions of ν for any θ, and are easily evaluated. The continued fractions $N_{2,-1}^1(\theta)$ and $P_{2,1}^1(\theta)$, defined by (A23) and (A24), are evaluated using the modified Lentz's method (see Sec. 5.2 in Ref. [34]). Both continued fractions usually converge within ten iterations when evaluated using this method. The root of $Z_2^1(\theta,\nu)$ is found using a simple bisection method. Although bisection may not be as efficient as other methods, it has the advantage that it is guaranteed to work once the root has been bracketed. This is helpful since we are interested in finding the root $\nu_2^1(\theta)$ of $Z_2^1(\theta,\nu)$ for many different θ; for some θ the root $\nu_2^1(\theta)$ lies *very* close to a singularity of $Z_2^1(\theta,\nu)$, and in these cases other root-finding methods may not converge (see Sec. 9.2 in Ref. [34]).

Once the characteristic exponent $\nu_2^1(\theta)$ has been calculated, the remaining problem is to calculate the sums (A20) of expansion coefficients $a_{2,r}^1(\theta)$ times Bessel functions $J_{\nu+2r+1/2}(2\theta^{1/2}z)$ and $Y_{\nu+2r+1/2}(2\theta^{1/2}z)$. The expansion coefficients are calculated using the continued fractions $N_{2,r}^1(\theta)$ and $P_{2,r}^1(\theta)$. With $a_{2,0}^1(\theta) = 1$, one has $a_{2,1}^1(\theta) = P_{2,1}^1(\theta)$, $a_{2,2}^1(\theta) = P_{2,2}^1(\theta) P_{2,1}^1(\theta)$, and in general

$$a_{2,n}^1(\theta) = \prod_{j=1}^{n} P_{2,j}^1(\theta). \tag{B2}$$

Likewise, the negative index expansion coefficients are given by

$$a_{2,-n}^1(\theta) = \prod_{j=1}^{n} N_{2,-j}^1(\theta). \tag{B3}$$

The continued fractions $N_{2,r}^1(\theta)$ and $P_{2,r}^1(\theta)$ are calculated using the modified Lentz's method as noted above. The normalization $s_2^1(\theta)$, defined in (A10), is calculated at the same time as the expansion coefficients.

The Bessel functions are calculated most efficiently using recurrence relations. The functions $J_{\nu+2r+1/2}(2\theta^{1/2}z)$ and $Y_{\nu+2r+1/2}(2\theta^{1/2}z)$ with $r \geq 0$ and $r < 0$ are handled separately. For $r \geq 0$, $J_{\nu+2r+1/2}(2\theta^{1/2}z)$ and $J_{\nu+2r+1/2-2}(2\theta^{1/2}z)$ are calculated for some large r using the routine BESSJY found in

[34]. Using the recurrence relations for Bessel functions (see 3.87 and 3.88 in [21]), the $J_{\nu+2r+1/2}(2\theta^{1/2}z)$ are calculated using downward recursion to $r = 0$ (this is the direction in which the recursion is stable for Bessel functions of the first kind [34]). A similar procedure, using upward recursion, is used for the Bessel functions of the second kind $Y_{\nu+2r+1/2}(2\theta^{1/2}z)$. This gives the necessary Bessel functions for $r \geq 0$.

The reflection formulas for Bessel functions are used to calculate the Bessel functions for $r < 0$. Since the index

$$\nu + 2r + 1/2 = -(2|r| - \nu - 1/2)$$

$$\text{for } r < 0 \text{ and } 1/2 < \nu < 3/2, \quad \text{(B4)}$$

the same procedure outlined above is used for $J_{2|r|-\nu-1/2}(2\theta^{1/2}z)$ and $Y_{2|r|-\nu-1/2}(2\theta^{1/2}z)$, and then the reflection formulas (see 6.7.19 of [34])

$$J_{-\upsilon}(y) = \cos\upsilon\pi J_{\upsilon}(y) - \sin\upsilon\pi Y_{\upsilon}(y), \quad \text{(B5)}$$

$$Y_{-\upsilon}(y) = \sin\upsilon\pi J_{\upsilon}(y) + \cos\upsilon\pi Y_{\upsilon}(y) \quad \text{(B6)}$$

are used to find $J_{\nu+2r+1/2}(2\theta^{1/2}z)$ and $Y_{\nu+2r+1/2}(2\theta^{1/2}z)$ for $r < 0$. So all the Bessel functions needed are calculated with only a few time-consuming calls to the routine BESSJY.

Once the expansion coefficients $a^1_{2,r}(\theta)$ and the Bessel functions $J_{\nu+2r+1/2}(2\theta^{1/2}z)$ and $Y_{\nu+2r+1/2}(2\theta^{1/2}z)$ are tabulated, the sums in (A20) are calculated. Care must be taken when terminating the sums. Although the expansion coefficients $a^1_{2,r}(\theta)$ fall off *very* quickly as $|r|$ becomes large, the products $a^1_{2,r}(\theta)J_{\nu+2r+1/2}(2\theta^{1/2}z)$ and $a^1_{2,r}(\theta)Y_{\nu+2r+1/2}(2\theta^{1/2}z)$ may not fall off as fast. We terminate the sums when the *products* of the expansion coefficients and Bessel functions no longer contribute (at double-precision accuracy) to the sums.

The primary numerical technique used to evaluate the multipole moments (5.2) is numerical integration. Both the integral over κ in (5.2) and the integral over x in (5.3) were done using a fifth-order embedded Runge-Kutta-Fehlberg algorithm with adaptive step size control [34]. Although formally the upper limit of the integral over κ extends to some very large $\kappa_{\max}$ (see Appendix C), we only integrated until the remaining contribution became negligible. The Bessel function with index $l + 1/2$ was evaluated with the routine BESSJY.

APPENDIX C: ULTRAVIOLET DIVERGENCE OF THE MULTIPOLE MOMENTS IN A GENERAL CURVED SPACE TIME

In this appendix, we correct an oversight from Allen and Koranda [2] in which we develop the formalism for calculating the CBR multipole moments in spatially flat FRW cosmology. In that paper, we inserted a mode function expansion of the metric perturbation operator into the Sachs-Wolfe formula for the fractional temperature perturbation $\delta T/T$. The Sachs-Wolfe formula, however, is only valid if the CBR photons propagating through the spacetime are small (or localized) relative to the length scale of curvature fluctuations on the spacetime. This requirement restricts the range of momentum to $k_{\text{gravity wave}} \lesssim k_{\text{photon}}$. As we show in this appendix, this implies that the integrals over graviton wave number that occur in the formulas for the multipole moments must be cut off at a maximum frequency. If the integrals over the wave number are not cut off, the formulas for the multipole moments are actually ultraviolet divergent.

We use Allen and Koranda [2] as a starting point. From Eqs. (2.65) and (2.67) of that reference for the multipole moments in a spatially flat FRW spacetime, one has

$$\langle a_l^2 \rangle = 4\pi^2(l-1)l(l+1)(l+2)\int_0^\infty k dk |I_l(k)|^2, \quad \text{(C1)}$$

where we have changed the definition of the function I, slightly, to

$$I_l(k) = \int_0^{\Delta\eta} d\lambda F(\lambda, k)\frac{j_l(k(\Delta\eta - \lambda))}{k^2(\Delta\eta - \lambda)^2}, \quad \text{(C2)}$$

with $\Delta\eta \equiv \eta_{\text{obs}} - \eta_e$, and $j_l(z)$ a spherical Bessel function. Define a new integration variable $s \equiv k(\Delta\eta - \lambda)$. Changing variables in the integral defining I one has

$$I_l(k) = \int_0^{k\Delta\eta} ds \frac{F(\Delta\eta - s/k, k)}{k}\frac{j_l(s)}{s^2}. \quad \text{(C3)}$$

We now show that in any reasonable spacetime, the functions $I_l(k)$ approach *nonzero constants* as $k \to \infty$. This means that the multipole moments are ultraviolet divergent.

The crucial point here is that as $k \to \infty$, all curved space mode functions take on flat spacetime behavior. This is because in the high-frequency limit, where the wavelengths are very short, the waves do not know that they are propagating in a curved spacetime. On small enough length scales any spacetime appears to be flat, and thus at high enough frequency, any normalized positive-frequency mode function approaches the form of the corresponding flat spacetime mode. Thus, up to an unimportant overall phase,

$$\lim_{k\to\infty} \phi(k,\eta) = \frac{\sqrt{\hbar G}}{\pi a(\eta)}\frac{e^{-ik\eta}}{\sqrt{k}}. \quad \text{(C4)}$$

The function F defined by $F(\lambda, k) = \sqrt{k}\dot{\phi}(k,\eta)|_{\eta_e+\lambda}$ has the following behavior at large k: As $k \to \infty$,

$$\frac{F(\Delta\eta - s/k, k)}{k} \to -i\frac{\sqrt{\hbar G}}{\pi a(\eta_{\text{obs}})}e^{-ik\eta_{\text{obs}}}e^{is}[1 + O(1/k)]. \quad \text{(C5)}$$

In calculating this last term, we have dropped terms of order $\dot{a}/a$, since for large enough k, they are smaller than the terms of order k that we have kept. This follows from our assumption that the wavelength is much shorter than the curvature radius of the spacetime. Thus as $k \to \infty$ one finds that (up to an unimportant overall phase which

might arise from the mode function)

$$\lim_{k\to\infty} I_l(k) \to -i\frac{\sqrt{\hbar G}}{\pi a(\eta_{\rm obs})} e^{-ik\eta_{\rm obs}} \int_0^{k\Delta\eta} ds \frac{e^{is}}{s^2} j_l(s). \quad \text{(C6)}$$

The overall phase in front of this expression may be dropped when calculating the multipole moments, which depend only upon $|I_l(k)|^2$. Hence the large k behavior of the integral is given by

$$\langle a_l^2 \rangle = 4\frac{\hbar G}{a^2(\eta_{\rm obs})}(l-1)l(l+1)(l+2)\int_0^\infty kdk \left| \int_0^{k\Delta\eta} ds \frac{e^{is}}{s^2} j_l(s) \right|^2 . \quad \text{(C7)}$$

To see that this quantity diverges at large k is straightforward. We note also that this expression is (at least formally) the exact flat Minkowski spacetime expression.

Consider the large k limit of $|I_l(k)|^2$. For general l this is given by

$$\int_0^\infty ds \frac{e^{is}}{s^2} j_l(s) = \frac{2i^{(l-1)}}{(l-1)l(l+1)(l+2)}. \quad \text{(C8)}$$

Because these integrals approach constant nonzero values as the upper limit increases, the integral which defines the multipole moments is infinite. If we take the upper limit of the k integral to be $k_{\rm max}$, then as this limit increases, one finds that the multipole moments diverge:

$$\begin{aligned}\langle a_l^2 \rangle &= \frac{4\hbar G}{a^2(\eta_{\rm obs})}(l-1)l(l+1)(l+2)\int_0^{k_{\rm max}} kdk \left| \int_0^{k\Delta\eta} ds \frac{e^{is}}{s^2} j_l(s) \right|^2 \\ &= \frac{8\hbar G}{a^2(\eta_{\rm obs})}\left[\frac{k_{\rm max}^2}{(l-1)l(l+1)(l+2)} + \frac{1}{2}\ln(k_{\rm max}) + \frac{1}{2}(\gamma + \ln 2 + 8) + 8\sum_{n=1}^{l}\frac{1}{n} \right] + O(k_{\rm max}^{-1}) \quad \text{for} \quad k_{\rm max} \gg 1, \quad \text{(C9)}\end{aligned}$$

where $\gamma = 0.5772\ldots$ is Euler's constant [see (6.1.3) of Ref. [30]]. Note that in this expression, the variable $k_{\rm max}$ is dimensionless. This is the exact Minkowski spacetime expression in the Lorentz vacuum state; it contains quadratic and logarithmic ultraviolet divergence as the cutoff $k_{\rm max} \to \infty$. As we have also shown, identical ultraviolet divergent behavior occurs in a general spacetime.

As a specific example, we show that this behavior occurs in the inflationary cosmological model constructed by Allen and Koranda in the reference above. We only need to demonstrate that the large k behavior of F corresponds to our formula above. To see that this is the case, we first note that as $k \to \infty$ one has $\alpha \to 1$ and $\beta \to 0$. Thus the mode function approaches $\phi^+_{\rm mat}$. One can see that for large k one has $h_1^{(2)}(kz) \to -e^{-ikz}/(kz)$ and that the various factors of η_1, η_2, $\rho_{\rm Planck}$, and $\rho_{\rm dS}$ appearing in the definition of $\phi^+_{\rm mat}$ combine to give

$$\lim_{k\to\infty} \phi^+_{\rm mat}(k,\eta) = ie^{-ik\eta_2}\frac{\sqrt{\hbar G}}{\pi a(\eta)}\frac{e^{-ik\eta}}{\sqrt{k}}. \quad \text{(C10)}$$

Thus in this specific example, the high-frequency behavior of the mode functions is exactly as assumed above—it approaches the flat space form for large k.

This divergence is fairly easy to understand and to remove. The explanation is obtained by considering the limits of applicability of the Sachs-Wolfe effect. The perturbations of the photon path and energy, described by the Sachs-Wolfe integral, are classical effects valid for wavelengths $\lambda_{\rm CBR} \le \lambda_{\rm graviton}$. Only when this inequality is satisfied may one treat the photon as a point particle propagating in a classical, curved background geometry. For gravitons of higher frequency, the effects of quantum gravity invalidate this approximation for the photon-graviton interaction. However, one can see on physical grounds that high-frequency graviton zero-point motion cannot significantly modify the multipole moments, because in ordinary laboratory experience, the propagation of electromagnetic microwave radiation is unaffected by graviton zero-point motion. Hence, we apply a physical cutoff $k_{\rm max} = 2\pi a(\eta_{\rm obs})/\lambda_{\rm CBR}$ to the mode number appearing in the Sachs-Wolfe formula. For observed wavelengths $\lambda_{\rm CBR} \sim 1$ cm, we obtain

$$\langle a_l^2 \rangle = \frac{\hbar G}{(\lambda_{\rm CBR})^2}\frac{32\pi^2}{(l+2)(l+1)l(l-1)} \approx 10^{-66}. \quad \text{(C11)}$$

Thus we obtain a reasonable, finite result for the CBR multipole moments in Minkowski spacetime, and for the high-frequency contribution to the multipole moments in a general curved spacetime.

[1] R.K. Sachs and A.M. Wolfe, Astrophys. J. **147**, 73 (1967).
[2] Bruce Allen and Scott Koranda, Phys. Rev. D **50**, 3713 (1994). Note that the caption for Table I of this reference should indicate that the multipoles listed in the table have been divided by $\rho_{\rm dS}/\rho_P$. The definition of M_l given in the caption of Fig. 2 contains a spurious factor of $\rho_{\rm dS}/\rho_P$; the correct definition is given by (5.5) of this paper. The integral over wave number in Eq. (2.67) should be cut off at some large $k_{\rm max}$ (see Appendix C). Finally, there is a sign error in the first term of Eq. (3.10). As a result the right-hand side of Eqs. (3.11)–(3.15) and (3.19) should have the opposite sign.
[3] V.A. Rubakov, M.V. Sazhin, and A.V. Veryaskin, Phys. Lett. **115B**, 189 (1982).
[4] R. Fabbri and M.D. Pollock, Phys. Lett. **125B**, 445 (1983).
[5] L.F. Abbott and M.B. Wise, Nucl. Phys. **B244**, 541 (1984); Phys. Lett. **135B**, 279 (1984).
[6] A. A. Starobinsky, Pis'ma Astron. Zh. **9**, 579 (1983) [Sov. Astron. Lett. **9**, 302 (1983)]; **11**, 323 (1985) [**11**, 133 (1985)].
[7] M. White, Phys. Rev. D **46**, 4198 (1992).
[8] L.P. Grishchuk, Phys. Rev. Lett. **70**, 2371 (1993); Class. Quantum Grav. **10**, 2449 (1993); Phys. Rev. D **48**, 3513 (1993); **48**, 5581 (1993); **46**, 1440 (1992).
[9] Michael S. Turner, Martin White, and James E. Lidsey, Phys. Rev. D **48**, 4613 (1993).
[10] K. Ng and A.D. Speliotopoulos, this issue, Phys. Rev. D **52**, 2112 (1995).
[11] Robert Crittenden, J. Richard Bond, Richard L. Davis, George Efstathiou, and Paul J. Steinhardt, Phys. Rev. Lett. **71**, 324 (1993).
[12] Scott Dodelson, Lloyd Knox, and Edward W. Kolb, Phys. Rev. Lett. **72**, 3444 (1994).
[13] Richard L. Davis, Hardy M. Hodges, George F. Smoot, Paul J. Steinhardt, and Michael S. Turner, Phys. Rev. Lett. **69**, 1856 (1992).
[14] Andrew R. Liddle and David H. Lyth, Phys. Lett. B **291**, 391 (1992).
[15] Francesco Lucchin, Sabino Matarrese, and Silvia Mollerach, Astrophys. J. **401**, L49 (1992).
[16] D.S. Salopek, Phys. Rev. Lett. **69**, 3602 (1992).
[17] Tarun Souradeep and Varun Sahni, Mod. Phys. Lett. A **7**, 3541 (1992).
[18] Lloyd Knox and Michael S. Turner, Phys. Rev. Lett. **73**, 3347 (1994).
[19] V. Sahni, Phys. Rev. D **42**, 453 (1990); Class. Quantum Grav. **5**, L113 (1988).
[20] H. Nariai, Prog. Theor. Phys. Suppl. **70**, 301 (1981).
[21] J.D. Jackson, *Classical Electrodynamics* (Wiley, New York, 1975).
[22] For a review of inflationary cosmology see E. Kolb and M. Turner, *The Early Universe* (Addison-Wesley, New York, 1990).
[23] B. Allen, Phys. Rev. D **37**, 2078 (1988).
[24] Martin White (private communication).
[25] Paul Steinhardt (private communication).
[26] S. Koranda, B. Allen, and P. Steinhardt, "A comparison between Boltzmann and Sachs-Wolfe treatments of gravitational wave induced CBR anisotropy," University of Wisconsin-Milwaukee and University of Pennsylvania report (unpublished).
[27] L.P. Grishchuk, Zh. Eksp. Teor. Fiz. **67**, 825 (1974) [Sov. Phys. JETP **40**, 409 (1975)]; L.H. Ford and Leonard Parker, Phys. Rev. D **16**, 245 (1977); **16**, 1601 (1977).
[28] *Higher Transcendental Functions*, edited by A. Erdélyi (Robert E. Krieger Publishing, Malabar, FL, 1981), Vol. 3.
[29] J. Meixner and F.W. Schäfke, *Mathieusche Funktionen und Sphäroidfunktionen, mit Anwendungen auf physikalische und technische Probleme* (Springer, Berlin, 1954).
[30] *Handbook of Mathematical Functions*, edited by M. Abramowitz and I. Stegun, Natl. Bur. Stand. Appl. Math. Ser. No. 55 (U.S. GPO, Washington, D.C., 1972).
[31] C. Flammer, *Spheroidal Wave Functions* (Stanford University Press, Stanford, CA, 1957); J.A. Stratton *et al.*, *Spheroidal Wave Functions, including Tables of Separation Constants and Coefficients* (Technology Press, Cambridge/Wiley, New York, 1956).
[32] P.M. Morse and H. Feshbach, *Methods of Theoretical Physics* (McGraw-Hill, New York, 1953).
[33] W. Gautschi, SIAM Rev. **9**, 24 (1967).
[34] William H. Press *et al.*, *Numerical Recipes in C*, 2nd ed. (Cambridge University Press, Cambridge, England, 1992).